UPPSALA
UNIVERSITET

Digital Comprehensive Summaries of Uppsala Dissertations from the Faculty of Science and Technology 699

Physics at the High-Energy Frontier

Phenomenological Studies of Charged Higgs Bosons and Cosmic Neutrino Detection

OSCAR STÅL

ACTA
UNIVERSITATIS
UPSALIENSIS
UPPSALA
2009

ISSN 1651-6214
ISBN 978-91-554-7682-3
urn:nbn:se:uu:diva-111162

Dissertation at Uppsala University to be publicly examined in Häggsalen, Ångströmlaboratoriet, Uppsala, Friday, January 29, 2010 at 13:15 for the Degree of Doctor of Philosophy. The examination will be conducted in English

Abstract

Stål, O. 2009. Physics at the High-Energy Frontier. Phenomenological Studies of Charged Higgs Bosons and Cosmic Neutrino Detection. Acta Universitatis Upsaliensis. *Digital Comprehensive Summaries of Uppsala Dissertations from the Faculty of Science and Technology* 699. 71 pp. Uppsala. ISBN 978-91-554-7682-3

The Standard Model of particle physics successfully describes present collider data. Nevertheless, theoretical and cosmological results call for its extension. A softly broken supersymmetric completion around the TeV scale solves several of the outstanding issues. Supersymmetry requires two Higgs doublets, leading to five physical Higgs states. These include a pair of charged Higgs bosons $H^{\pm}$, which are a generic feature of theories with multiple Higgs doublets.

Using results from high-energy colliders and flavour physics, constraints are derived on the charged Higgs boson mass and couplings; both for constrained scenarios in the minimal supersymmetric standard model (MSSM) with grand unification, and for general two-Higgs-doublet models. The MSSM results are compared to the projected reach for charged Higgs searches at the Large Hadron Collider (LHC). At the LHC, a light charged Higgs is accessible through top quark decay. Beyond a discovery, it is demonstrated how angular distributions sensitive to top quark spin correlations can be used to determine the structure of the $H^{\pm}tb$ coupling. The public code `2HDMC`, which performs calculations in a general, CP-conserving, two-Higgs-doublet model, is introduced.

In parallel to the developments at colliders, the most energetic particles ever recorded are the ultra-high-energy (UHE) cosmic rays. To gain more insight into their origin, new experiments are searching for UHE neutrinos. These searches require detectors of vast volume, which can be achieved by searching for coherent radio pulses arising from the Askaryan effect. The prospects of using a satellite orbiting the Moon to search for neutrino interactions are investigated, and a similar study for an Earth-based radio telescope is presented. In both cases, the method is found competitive for detection of the very highest energy neutrinos considered.

Keywords: particle physics, Standard Model, beyond the Standard Model, supersymmetry, Higgs physics, charged Higgs boson, LHC, flavour physics, ultra-high-energy neutrinos, Askaryan effect, radio detection, lunar satellites

Oscar Stål, Department of Physics and Astronomy, Uppsala University, Box 516, SE-751 20 Uppsala, Sweden

ISSN 1651-6214
ISBN 978-91-554-7682-3
urn:nbn:se:uu:diva-111162 (http://urn.kb.se/resolve?urn=urn:nbn:se:uu:diva-111162)

Optimis parentibus

List of Papers

This thesis is based on the following papers, which are referred to in the text by their Roman numerals.

I D. Eriksson, F. Mahmoudi, O. Stål, Charged Higgs bosons in minimal supersymmetry: updated constraints and experimental prospects, *JHEP* **0811** (2008) 035, [arXiv:0808.3551] [hep-ph].

II O. Stål, Constraints on charged Higgs bosons in the CMSSM and NUHM models, *In proceedings of cHarged 2008*, *PoS(CHARGED2008)* (2008) 021.

III D. Eriksson, J. Rathsman, O. Stål, 2HDMC – two-Higgs-doublet model calculator, *Computer Physics Communications* **181** (2010) 189, [arXiv:0902.0851] [hep-ph].

IV F. Mahmoudi, O. Stål, Flavor constraints on two-Higgs-doublet models with general diagonal Yukawa couplings, *Submitted* (2009), [arXiv:0907.1791] [hep-ph].

V O. Stål, Constraints on the two-Higgs-doublet model, *Submitted to the proceedings of SUSY09* (2009), [arXiv:0909.5031] [hep-ph].

VI D. Eriksson, G. Ingelman, J. Rathsman, O. Stål, New angles on top quark decay to a charged Higgs, *JHEP* **0801** (2008) 024, [arXiv:0710.5906] [hep-ph].

VII O. Stål, New angles on top quark decay to a charged Higgs boson, *In proceedings of TOP2008, Nuovo Cimento* **123B** (2008) 1211, [arXiv:0809.0980] [hep-ph].

VIII O. Stål, J.E.S Bergman, B. Thidé, L.K.S. Daldorff, G. Ingelman, Prospects for Lunar Satellite Detection of Radio Pulses from Ultrahigh Energy Neutrinos Interacting with the Moon, *Physical Review Letters* **98** (2007) 071103, [astro-ph/0604199].

IX S. Panda, S. Mohanty, P. Janardhan, O. Stål, Prospects for the Giant Metrewave Radio Telescope to observe radio waves from ultra high energy particles interacting with the Moon, *JCAP* **0711** (2007) 022, [arXiv:0708.1683] [astro-ph].

Contents

Introduction

Particle physics is the science of identifying the fundamental building blocks of matter and the interactions taking place between them. It is fair to say that this has been an extremely successful endeavour over the last century. The gathered knowledge has culminated in the Standard Model, which explains the present experimental results to excellent precision. Now, on the eve before the Large Hadron Collider (LHC) starts to deliver data, we ask what lies beyond the Standard Model? The question is asked with confidence, knowing that consistency of the theory suggests that something new should show up to save the day when the high-energy frontier is pushed yet another step forward.

The Standard Model still contains one undiscovered particle: the Higgs boson. To find it is a major objective for the LHC. Instead of an end, this might mark the beginning of experimental Higgs physics, since well-motivated extensions of the Standard Model (e.g. supersymmetry) contain additional Higgs bosons. Supersymmetry, and in fact all non-trivial extensions of the Higgs sector, predict that two of these make up an electrically charged pair $H^{\pm}$. Since this charged Higgs boson cannot be confused with the ordinary one, which is electrically neutral, its discovery would be an unambiguous sign of physics beyond the Standard Model. A major part of this thesis is devoted to the phenomenology of charged Higgs bosons.

In parallel to the development of the Standard Model from results obtained primarily at colliders, the true high-energy frontier of physics is observed in the highest energy cosmic rays continuously bombarding the Earth. This high-energy branch of astroparticle physics has recently been extended with experiments designed to detect cosmic neutrinos. The best limits on the neutrino flux in the highest energy regime are held by experiments searching for coherent radio emission produced through the Askaryan effect. Simulation studies of the prospects for new experiments of this type with the Moon as neutrino target are presented as the second topic of this thesis.

The thesis is organized as follows: in chapter 1 we give a theoretical introduction to the Standard Model of particle physics. We then proceed in chapter 2 with its minimal supersymmetric extension (MSSM), focusing in particular on the Higgs sector and constrained models which are used for phenomenology. In chapter 3 the MSSM Higgs sector is placed in the wider context of general two-Higgs-doublet models. As already alluded to, a main topic of this thesis is going to be the phenomenology of charged Higgs bosons. It is therefore discussed in two chapters: chapter 4, which contains material

of relevance for charged Higgs searches at high-energy colliders, and chapter 5, where some of the most important low-energy observables sensitive to charged Higgs exchange are discussed. Finally, chapter 6 contains an introduction to the second topic, cosmic neutrino detection with radio methods. Readers feeling overwhelmed already by this introduction may skip straight to the Swedish summary on page 59.

1. The Standard Model

> "I'm a physicist. I have a working knowledge of the entire universe and everything it contains."
>
> Sheldon Cooper

This chapter introduces the Standard Model (SM) of particle physics as a renormalizable quantum field theory based on local gauge invariance under the group $\mathrm{SU}(3) \times \mathrm{SU}(2) \times \mathrm{U}(1)$. The strong and electroweak interactions are described at the principal level. Massive gauge bosons are introduced through spontaneous symmetry breaking of $\mathrm{SU}(2) \times \mathrm{U}(1)$ via the Higgs mechanism, which is also responsible for generating fermion masses. Since the work on which this thesis is based to a large extent deals with extensions of the Standard Model, so-called *new physics*, the last section of this chapter provides motivation for such extensions by describing a few different shortcomings of the model.

1.1 Perturbative gauge theory

To introduce the important notion of local gauge invariance, we first discuss the example of an Abelian U(1) symmetry. Physically this corresponds to the theory of Quantum Electrodynamics (QED). Starting from the *Lagrangian* density

$$\mathcal{L}_0 = \overline{\psi}(x)\left(\mathrm{i}\gamma^\mu \partial_\mu - m\right)\psi(x), \tag{1.1}$$

which describes a free fermion field $\psi(x)$, this is seen to be invariant under a global U(1) gauge transformation

$$\psi(x) \to \psi'(x) = e^{-\mathrm{i}q\,\theta}\psi(x). \tag{1.2}$$

Making the transformation *local*, by allowing θ to depend on the space-time coordinate $\theta \to \theta(x)$, the derivative term in equation (1.1) is no longer invariant but

$$\partial_\mu\left(e^{-\mathrm{i}q\theta(x)}\psi(x)\right) = e^{-\mathrm{i}q\theta(x)}\partial_\mu\psi - \mathrm{i}q\left[\partial_\mu\theta(x)\right]e^{-\mathrm{i}q\theta(x)}\psi. \tag{1.3}$$

The way to remedy the situation and restore gauge invariance is by introducing a vector *gauge field* $A_\mu(x)$. Utilizing this new field, we can write a covariant derivative as

$$D_\mu = \partial_\mu - i g q A_\mu(x). \tag{1.4}$$

This derivative is covariant in the sense that, under a U(1) transformation, it should transform in the same way as the field ψ itself. In other words

$$D_\mu \psi \to \left(D_\mu \psi\right)' = e^{-\mathrm{i}q\theta(x)} D_\mu \psi, \tag{1.5}$$

which is realized when the gauge field simultaneously transforms as

$$A_\mu \to A'_\mu = A_\mu - \frac{1}{g}\partial_\mu \theta(x). \tag{1.6}$$

Substituting the ordinary derivative in equation (1.1) with the covariant derivative we obtain

$$\mathcal{L} = \overline{\psi}(x)\left(\mathrm{i}\gamma^\mu \partial_\mu + g q \gamma^\mu A_\mu(x) - m\right)\psi(x), \tag{1.7}$$

which now describes a theory where the ψ fields interact via the A_μ field. The overall strength of the interaction is given by the gauge *coupling* g. The gauge field is made dynamical by adding to equation (1.7) the term

$$\mathcal{L} = -\frac{1}{4} F_{\mu\nu} F^{\mu\nu}, \tag{1.8}$$

where $F_{\mu\nu} = \partial_\mu A_\nu - \partial_\nu A_\mu$ is the electromagnetic field strength tensor.

A general non-Abelian gauge theory describes a set of vector fields A^a_μ transforming under the adjoint representation of the corresponding gauge group.[1] In analogy to equation (1.4), each interaction has its associated gauge-covariant derivative

$$D_\mu = \partial_\mu - \mathrm{i}g T^a A^a_\mu, \tag{1.9}$$

where T^a are the generators of the group, $[T^a, T^b] = \mathrm{i} f^{abc} T^c$ defines the structure constants f^{abc}, and g is the corresponding gauge coupling. The covariant derivative generates couplings of the gauge fields to fermions and scalars. The curvature, or field strength, tensor now reads

$$F^a_{\mu\nu} \equiv \frac{\mathrm{i}}{g}\left[D_\mu, D_\nu\right]^a = \partial_\mu A^a_\nu - \partial_\nu A^a_\mu + g f^{abc} A^b_\mu A^c_\nu. \tag{1.10}$$

[1]The number of gauge bosons A^a_μ mediating each interaction is therefore equal to the number of generators of the group, e.g. $N^2 - 1$ for SU(N).

Analogous to equation (1.8), one constructs from the field strength the Yang-Mills term [1]

$$\mathcal{L}_{\mathrm{YM}} = -\frac{1}{4}\mathrm{Tr}\left(F_{\mu\nu}F^{\mu\nu}\right), \tag{1.11}$$

where the trace is taken over the group space. As may be readily verified by expanding equation (1.11), a non-Abelian gauge symmetry leads to terms with three and four gauge fields. These gauge field self-interactions have important phenomenological implications, in particular for the strong interaction as we shall see in the next section. Note also that explicit mass terms for the gauge fields are not invariant under a gauge transformation. The gauge theory thus describes massless gauge bosons.

The Lagrangian defines the field theory at the classical level, and the classical equations of motion are given by the Euler-Lagrange equations. By quantizing the excitations of the field (e.g. using the path-integral formalism [2]) it is turned into a quantum field theory. The quantization yields the propagators of the theory and Feynman rules for the interactions. To derive expressions for the gauge field propagators, the gauge must be fixed to avoid integration over equivalent field configurations. This is usually achieved by adding a gauge-fixing term

$$\mathcal{L}_{\mathrm{GF}} = -\frac{1}{2\xi}\left(\partial^{\mu}A_{\mu}\right)^2 \tag{1.12}$$

to the classical Lagrangian, where different values of ξ correspond to different choices of gauge. The end result of a gauge-invariant computation is independent of ξ. When quantizing a non-Abelian gauge theory, an additional complication is that certain gauges require the introduction of *ghost* fields [3] to cancel contributions from unphysical degrees of freedom which appear in loop calculations.

Most calculations in a quantum field theory proceed using perturbative methods. An observable $\mathcal{O} \sim |\mathcal{M}|^2$ (e.g. a cross section), calculated from the matrix element $\mathcal{M}$, is then expressed as a power series in the coupling

$$\mathcal{O} = C_1 g^2 + C_2 g^4 + C_3 g^6 + \ldots \tag{1.13}$$

In a theory where the coupling g is small, this is a convergent procedure in which the higher orders of the perturbative series can be truncated. The perturbative series is represented by *Feynman diagrams* of increasing complexity, where each additional vertex contributes a factor g to the amplitude. Examples of these diagrams are shown in figure 1.1.

When calculating loop diagrams, internal loop momenta are not constrained by momentum conservation, and integrals over these unconstrained momenta can become infinite. *Renormalization* is a prescription for dealing with these divergences systematically by absorbing them into shifts of the parameters (couplings, masses) of the theory. The physical (renormalized) parameters are

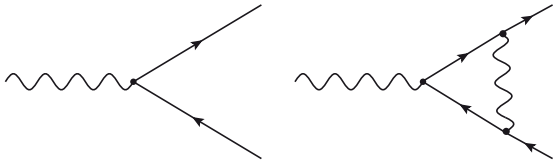

Figure 1.1: Feynman diagrams for a tree-level interaction (left) and a one-loop correction (right). Solid lines indicate fermions and the wavy lines gauge bosons (photons).

thus not the same as the bare (original) parameters in the Lagrangian. Theories which allow all divergences to be absorbed through a finite number of redefinitions in this way are said to be *renormalizable*. This property is essential for a predictive quantum field theory. A simple way to check renormalizability directly from the Lagrangian is to investigate the mass dimension of the operators. Renormalizable operators have at most dimension four (in four dimensional space-time). The procedure of renormalization introduces an arbitrary dimensionful parameter, the *renormalization scale* μ_{R}. The renormalized parameters depend on this scale through *renormalization group equations* (RGE). The coupling $g(\mu_{\mathrm{R}})$ is then said to be running.

1.2 Quantum chromodynamics

Quantum chromodynamics (QCD) is the theory of the strong interaction which acts on *quarks*, the fundamental constituents of hadronic matter. It is described by the unbroken gauge group of *colour*, denoted by $\mathrm{SU}(3)_C$. The eight gauge bosons are called *gluons*. At first sight, QCD as a gauge theory has one dimensionless parameter: the coupling $\alpha_s = g_s^2/4\pi$. However, as we shall see below, a dynamical scale is introduced from the renormalization of the coupling. Furthermore, via the addition of massive fermions, it becomes a multi-scale theory.

The QCD coupling at low (hadronic) energy scales is large. It is only by incorporating radiative corrections through the renormalization group that the applicability of perturbative QCD at higher energies can be understood. The evolution of α_s with the scale μ^2 is described by the renormalization group equation

$$\mu^2 \frac{\partial \alpha_s}{\partial \mu^2} = \beta(\alpha_s), \tag{1.14}$$

where the β-function is given by a perturbative expansion in α_s

$$\beta(\alpha_s) = -\alpha_s \sum_{n=0}^{\infty} \beta_n \left(\frac{\alpha_s}{4\pi}\right)^{n+1}. \tag{1.15}$$

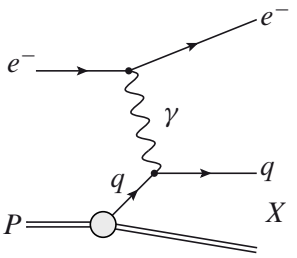

Figure 1.2: Leading order deep-inelastic $e^- p$ scattering.

This function is, in principle, calculable to arbitrary order. It is known up to four loops [4], but we content ourselves with the leading order coefficient

$$\beta_0 \equiv 4\pi b_0 = 11 - \frac{2}{3} n_f . \tag{1.16}$$

In this expression, n_f is the number of *active* (light) quark flavours. As a result of the gluon self-coupling, the leading coefficient of the QCD β-function is negative for $n_f \leq 16$. This behaviour persists at higher orders. The coupling is thus expected to decrease in magnitude with increasing μ^2, a property known as *asymptotic freedom* [5]. Using β_0 as input, we may solve equation (1.14) to relate the running coupling at two separate scales

$$\alpha_s\left(\mu^2\right) = \frac{\alpha_s\left(\mu_0^2\right)}{1 + b_0 \alpha_s\left(\mu_0^2\right) \log\left(\mu^2/\mu_0^2\right)}. \tag{1.17}$$

Due to the running of α_s, a dynamical scale $\Lambda_{\mathrm{QCD}} \sim 200$ MeV is generated where $\alpha_s \to \infty$. The appearance of this scale signals the transition to a strongly coupled theory where hadrons, rather than quarks and gluons, are the relevant degrees of freedom. This property of QCD is called *confinement*.

Because of confinement, quarks and gluons are only observed as *partons* inside hadrons and never as free particles at low energy (large spatial separation). The parton structure of the proton is described by universal *parton distribution functions* $f_i(x)$. These functions receive contributions from non-perturbative QCD, and can thus not be calculated from first principles. Through *factorization*, a process formally similar to renormalization, collinear divergences are absorbed into the unobservable, bare, parton distributions. Like renormalization, this introduces a scale dependence of the redefined distributions: $f_i(x) \to f_i\left(x, \mu_{\mathrm{F}}^2\right)$. The corresponding factorization scale μ_{F} is an arbitrary parameter chosen to separate physics taking place at short and long distances.[2] What makes the factorization approach useful is that the scale de-

[2]Note that the factorization scale μ_{F} must not necessarily equal the renormalization scale μ_{R}, introduced to deal with UV divergences. To avoid large logarithms in calculations, both scales should be chosen as some scale in the physical process. In many cases, a common scale $\mu_{\mathrm{F}} = \mu_{\mathrm{R}} = \mu$ is both physically motivated and convenient.

pendence of $f_i\left(x,\mu_{\mathrm{F}}^2\right)$ can be calculated perturbatively through the DGLAP equations [6]. Schematically, for one parton type k, the equation reads

$$\frac{\partial}{\partial \ln \mu_{\mathrm{F}}^2} f_i\left(x,\mu_{\mathrm{F}}^2\right) = \frac{\alpha_s}{2\pi} \sum_i \int_x^1 \frac{\mathrm{d}\xi}{\xi} P_{k\to ij}\left(\frac{x}{\xi}\right) f_k(\xi,\mu_{\mathrm{F}}^2). \tag{1.18}$$

$P_{k\to ij}$ are here the regularized *splitting functions*, describing the splitting of a parton k into a pair of new partons i, j. Using a set of equations like (1.18), the parton distributions can be evolved from a reference scale to the relevant scale of the process at hand. Parton distributions for the proton may thus be extracted from global fits to QCD processes, such as deep-inelastic $e^- p$ scattering as depicted in figure 1.2, or fixed-target experiments.

1.3 Electroweak theory

Electroweak (EW) theory [7] is described by the combined $\mathrm{SU}(2)\times\mathrm{U}(1)$ symmetry of the Standard Model. The three gauge fields of *weak isospin* $\mathrm{SU}(2)_L$ are denoted by A_μ^a $(a=1,2,3)$, and the gauge field of the Abelian *hypercharge* $\mathrm{U}(1)_Y$ by B_μ. The two couplings are g for $\mathrm{SU}(2)_L$ and g' for $\mathrm{U}(1)_Y$. The covariant derivative acting on a doublet of $\mathrm{SU}(2)_L$ is then given by

$$D_\mu = \partial_\mu - \mathrm{i}g\frac{\sigma^a}{2}A_\mu^a - \mathrm{i}\frac{g'}{2}YB_\mu, \tag{1.19}$$

where σ^a are the Pauli matrices. The Y quantum numbers are in general different for each field on which D_μ acts. The quantization of hypercharges (or for that matter, the electric charges) is not explained within the Standard Model.

Of the four observed electroweak gauge bosons, only one (the photon) is massless, whereas both $W^\pm$ and Z^0 are massive. The gauge symmetry $\mathrm{SU}(2)_L\times\mathrm{U}(1)_Y$ must thus be broken in a pattern $\mathrm{SU}(2)_L\times\mathrm{U}(1)_Y\to\mathrm{U}(1)_{\mathrm{EM}}$. Breaking the gauge symmetry explicitly by adding mass terms for the gauge bosons is not compatible with renormalizability [8], suggesting that the symmetry is instead spontaneously broken.[3] Counting degrees of freedom, at least three must be added to provide the longitudinal parts of the gauge fields, turning them into massive spin-1 fields. The most economical choice is to introduce a complex scalar doublet Φ [9], which also allows gauge-invariant mass terms for the fermions as will be shown in section 1.4. The unbroken electroweak Lagrangian, including the new scalar field Φ, reads

$$\mathcal{L}_{\mathrm{EW}} = -\frac{1}{4}\mathrm{Tr}\left(F^{\mu\nu}F_{\mu\nu}\right) - \frac{1}{4}B^{\mu\nu}B_{\mu\nu} + D^\mu\Phi^\dagger D_\mu\Phi - \mathcal{V}\left(|\Phi|^2\right). \tag{1.20}$$

[3] Spontaneous symmetry breaking occurs when a symmetry of the Lagrangian is not a symmetry of the vacuum state.

Requiring gauge invariance and renormalizability leads to the simple form

$$\mathcal{V}\left(|\Phi|^2\right) = m^2|\Phi|^2 + \lambda|\Phi|^4 \tag{1.21}$$

for the scalar potential. A stable vacuum configuration as $|\Phi| \to \infty$ requires $\lambda > 0$. When $m^2 < 0$, the potential has degenerate global minima for $|\Phi|^2 = -m^2/(2\lambda) \equiv v^2/2$. The value $\langle\Phi\rangle$ at the minimum is called the *vacuum expectation value*. Choosing an orientation in field space for the physical vacuum (the electrically neutral direction) breaks the electroweak symmetry spontaneously. By convention, a real and positive value for the lower component of the $Y = 1$ doublet is chosen, hence

$$\langle\Phi\rangle = \frac{1}{\sqrt{2}}\begin{pmatrix} 0 \\ v \end{pmatrix}. \tag{1.22}$$

This choice gives the electric charge operator $Q = T_3 + \frac{Y}{2}$, where T_3 is the third component of the weak isospin. The full scalar doublet can now be written in components as

$$\Phi(x) = \frac{1}{\sqrt{2}}\begin{pmatrix} \phi^+(x) \\ v + \phi^0(x) \end{pmatrix} = e^{\mathrm{i}\sigma^a G^a(x)}\begin{pmatrix} 0 \\ \frac{1}{\sqrt{2}}[v + h(x)] \end{pmatrix}. \tag{1.23}$$

The second parameterization makes it evident that the three scalar degrees of freedom $G^a(x)$ can be removed by a suitable local SU(2) gauge transformation (unitary gauge). Expanding the kinetic terms for Φ in equation (1.20) around the minimum, masses are generated for the gauge fields according to

$$W_\mu^\pm = \frac{1}{\sqrt{2}}\left(A_\mu^1 \mp \mathrm{i}A_\mu^2\right), \quad m_W^2 = \frac{1}{4}g^2v^2 \tag{1.24a}$$

$$Z_\mu^0 = \frac{gA_\mu^3 - g'B_\mu}{\sqrt{g^2 + g'^2}}, \quad m_Z^2 = \frac{1}{4}\left(g^2 + g'^2\right)v^2 \tag{1.24b}$$

$$A_\mu = \frac{g'A_\mu^3 + gB_\mu}{\sqrt{g^2 + g'^2}}, \quad m_\gamma^2 = 0. \tag{1.24c}$$

The relation to the known values of m_W or m_Z fixes the numerical value of $v = 246$ GeV. The neutral components can be more easily related by introducing the weak mixing angle

$$\sin\theta_W = \frac{g'}{\sqrt{g^2 + g'^2}}. \tag{1.25}$$

As a final remark on the weak gauge bosons, note the important relation

$$\rho \equiv \frac{m_W^2}{m_Z^2\cos^2\theta_W} = 1. \tag{1.26}$$

Field	$SU(3)_C$	$SU(2)_L$	$U(1)_Y$
$q_L = (u_L, d_L)^T$	**3**	**2**	$+1/3$
u_R	**3**	**1**	$+4/3$
d_R	**3**	**1**	$-2/3$
$\ell_L = (\nu_L, e_L)^T$	**1**	**2**	-1
e_R	**1**	**1**	-2

Table 1.1: *One generation of fermions in the Standard Model, with* U(1) *hypercharges and representations under* $SU(3)_C$ *and* $SU(2)_L$.

This is an exact tree-level identity, modified only by small radiative corrections. The precise experimental verification of this relation is one of the remarkable successes of the Standard Model. Results on the ρ parameter are accurate enough that any theory extending the electroweak sector in principle must preserve $\rho = 1$ at tree-level.

The final ingredient of the electroweak theory is the remaining degree of freedom $h(x)$ present in equation (1.23). This is the *Higgs boson*. Its mass is dictated by the scalar potential (1.21) to be

$$m_h^2 = 2\lambda v^2. \tag{1.27}$$

However, since λ is arbitrary, m_h is a free parameter that must be determined from experiment. Combining all the electroweak data gives the best fit $m_h = 87^{+35}_{-26}$ GeV [10]. There is a slight tension between this fit and the direct search results which exclude $m_h < 114.4$ GeV [11] at the 95% confidence level (CL). Including the direct search results in the fit, a one-sided upper limit on the Higgs mass is $m_h < 186$ GeV at 95% CL. The allowed mass window is further narrowed by the recent Tevatron results [12], excluding the range 163 GeV $< m_h <$ 166 GeV. As will be discussed further in section 1.5, not only is the experimental situation on the Higgs mass intriguing, but there are also theoretical issues related to m_h hinting at the existence of physics beyond the Standard Model.

1.4 Fermion masses

The Standard Model contains three generations of chiral fermions.[4] The left-chiral fields come in doublet representations of $SU(2)_L$, while the right-chiral fields are weak singlets. The transformation properties of the different fermions under the gauge symmetries are presented in table 1.1. As

[4]Chiral fields are eigenstates of the projectors $P_{R,L} = (1 \pm \gamma_5)/2$. In the case of massless fields, eigenstates of the helicity operator $h \equiv \vec{S} \cdot \hat{p}$ are also states of definite chirality. This is *not* the case for massive states.

can be seen from the table, each generation is incomplete; the right-handed neutrino ν_R is missing. Should this state exist, it must be a gauge singlet.

Due to the different transformation properties of the left-handed and right-handed fields, fermion mass terms $\mathcal{L}_m = -m_f(\overline{\psi}_L\psi_R + \overline{\psi}_R\psi_L)$ do not preserve gauge invariance. This is where the scalar doublet introduced to break the EW symmetry demonstrates its value. Since Φ is a doublet under $\mathrm{SU}(2)_L$, a mass term for each fermion can be generated by a *Yukawa coupling* to the scalar field. For the single generation of fermions introduced in table 1.1 this becomes

$$-\mathcal{L}_{\text{Yukawa}} = y_d\overline{q}_L\Phi d_R + y_u\overline{q}_L\widetilde{\Phi}u_R + y_\ell\overline{\ell}_L\Phi e_R + \text{h.c.}, \tag{1.28}$$

where $\widetilde{\Phi} = \mathrm{i}\sigma_2\Phi^*$ has hypercharge $Y = -1$. When the EW symmetry is spontaneously broken, Φ is replaced by its vacuum expectation value, and each fermion acquires a mass

$$m_f = y_f\frac{v}{\sqrt{2}}. \tag{1.29}$$

There is no symmetry in the Standard Model explaining the observed hierarchy in the Yukawa couplings; each coupling is a new parameter of the theory. Including all the three known fermion generations, the Lagrangian (1.28) gets modified into

$$-\mathcal{L}_{\text{Yukawa}} = \overline{Q}_L Y_D\Phi D_R + \overline{Q}_L Y_U\widetilde{\Phi}U_R + \overline{L}_L Y_L\Phi E_R + \text{h.c.}, \tag{1.30}$$

where Q, L, U, D and E are now three-component vectors in flavour space, e.g. $U = (u,c,t)^T$, $D = (d,s,b)^T$, and $E = (e,\mu,\tau)^T$. Consequently the Yukawa couplings Y_U, Y_D, and Y_L are 3×3 (complex) matrices. To identify the physical mass eigenstates, one performs unitary transformations on the fermion fields. The down-quark mass matrix is diagonalized by two matrices V_L^D and V_R^D such that

$$M_D = \frac{v}{\sqrt{2}}(V_L^D)^\dagger Y_D V_R^D, \tag{1.31}$$

and similarly for M_U. The charged current eigenstates do not coincide with the mass eigenstates, but a remnant flavour structure $V_{\text{CKM}} = (V_L^U)^\dagger V_L^D$ is left in the quark current coupling to $W_\mu^\pm$. This is the Cabibbo–Kobayashi–Maskawa (CKM) matrix [13, 14]. Being a product of unitary matrices, the CKM matrix is itself unitary. Any 3×3 unitary matrix is completely determined by three angles and one complex phase. The possibility to have a physically relevant phase – and thereby violation of the discrete $\mathcal{CP}$ symmetry[5] – requires at least three quark generations [14]. A necessary and sufficient con-

[5] $\mathcal{CP}$ invariance of an observable implies that it is unaffected by the consecutive application of the $\mathcal{P}$ (parity) and $\mathcal{C}$ (charge conjugation) transformations. Violation of $\mathcal{CP}$ is equivalent to a violation of $\mathcal{T}$ (time reversal), since the combined symmetry $\mathcal{CPT}$ must hold in a Lorentz-invariant theory.

dition for $\mathcal{CP}$ violation in the Standard Model may be written [15] in the mass eigenstate basis as

$$\begin{aligned}&(m_t^2 - m_c^2)(m_t^2 - m_u^2)(m_c^2 - m_u^2)\\ &\times (m_b^2 - m_s^2)(m_b^2 - m_d^2)(m_s^2 - m_d^2)\mathcal{J} \neq 0,\end{aligned} \tag{1.32}$$

where the $\mathcal{J}$ parameter is related to products of CKM matrix elements. Measurements are compatible with a non-zero value for $\mathcal{J}$ as the only source for $\mathcal{CP}$ violation.

The conclusive evidence for neutrino oscillations [16] implies that neutrinos are massive, contrary to what was originally assumed. This leads to the introduction of similar structure in the lepton sector as for the quarks. Introducing a right-handed neutrino N_R allows the ordinary Yukawa mass term, cf. equation (1.28), for one neutrino flavour

$$-\mathcal{L}^{\nu}_{\text{Yukawa}} = y_\nu \overline{\ell}_L \Phi N_R + \text{h.c.} \tag{1.33}$$

With miniscule values for y_ν, this term gives neutrino masses $m_\nu = y_\nu v/\sqrt{2}$ in the same way as the other Yukawa couplings. However, since N_R is a gauge singlet, another option exists. For the case of a single neutrino flavour, a Majorana mass term reads

$$-\mathcal{L}^{\nu}_{\text{Majorana}} = \frac{1}{2} M \overline{N}^c_L N_R + \text{h.c.} \tag{1.34}$$

The new mass parameter M has no relation to electroweak symmetry breaking and may therefore be arbitrarily large ($M \gg v$). The neutrino mass eigenstates are obtained by combining the two mass terms in a matrix and performing a diagonalization. When $M \gg m_\nu$, the mass eigenvalues are $m_1 \sim M$ and $m_2 \sim m_\nu^2/M$, showing that m_2 can become very small [17]. This is called the *seesaw mechanism*. To get the experimentally observed range for the neutrino masses when $m_\nu \sim v$ requires $M \simeq 10^{13}$ GeV. In analogy to the CKM matrix in the quark sector, neutrino mixing is described by a unitary matrix $V = (V_L^\nu)^\dagger V_L^\ell$. Unless massive neutrinos are implied by the context (as in parts of the discussion in chapter 6), we assume them to be massless in the following. For most purposes this is an excellent approximation.

1.5 Shortcomings of the Standard Model

Calling the Standard Model a successful theory would be an understatement. The theory has been tested at LEP to better than one percent precision, and no significant deviations are observed (see e.g. the global fit performed by the Particle Data Group [18]). Nevertheless, there are a number of indications,

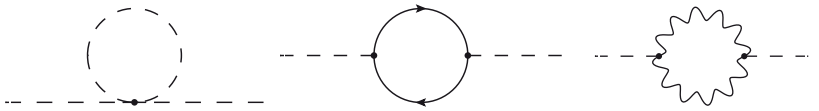

Figure 1.3: Scalar, fermion and gauge boson loop diagrams which generate quadratically divergent contributions to the mass of the Higgs boson.

hints, and theoretical prejudice all pointing to the fact that the Standard Model needs to be embedded into a larger theory.

One important limitation involves the quantum corrections to the Higgs mass m_h. When these are calculated, diagrams such as those in figure 1.3 introduce quadratic divergences. If the divergent one-loop integrals are regularized using a physical cutoff scale Λ – corresponding to the scale at which new physics should appear – one obtains the correction

$$\delta m_h^2 = \frac{3\Lambda^2}{8\pi^2 v^2}\Big(4m_t^2 - 2m_W^2 - m_Z^2 - m_h^2\Big). \tag{1.35}$$

Note that fermions contribute positively, while the bosonic contributions to δm_h^2 are negative. Since $\delta m_h^2 \propto \Lambda^2$, a low Higgs mass in agreement with the experimental data is not stable with respect to a large scale Λ comparable to the Planck or grand unification scale. This conflict of scales is known as the *hierarchy problem*. The only way to preserve a low Higgs mass in the Standard Model is by adjusting the bare value of m_h to (almost) cancel the right-hand side of equation (1.35). However, this involves extreme fine-tuning and therefore corresponds to an *unnatural* solution of the hierarchy problem.[6] One may be tempted by equation (1.35) to arrange $m_h^2 = 4m_t^2 - 2m_W^2 - m_Z^2$ (known as the Veltman condition [19]) to avoid the quadratic divergence altogether. Unfortunately, this would only result in short euphoria, as revealed by calculating the next order in perturbation theory. In the next chapter, we shall see how a supersymmetric extension of the Standard Model provides a natural solution of the hierarchy problem.

A fundamental limitation of the Standard Model is that it does not contain a description of the gravitational force. Gravity, which has important phenomenological implications for everyday life, has so far not been successfully described as a renormalizable quantum field theory. For particle physics this has limited implications, as quantum gravity effects are only expected to become important in the description of phenomena at energy scales of order

[6] An unnatural solution is *not* the same as an impossible solution. For a theory to be natural in the technical sense simply means that observable quantities should be stable under small variations of the parameters. Naturalness suggests a symmetry principle behind any parameter that is small (or large) with respect to the fundamental scale. Small fermion masses are natural, since chiral symmetry is restored for $m_f = 0$.

$M_{\rm P} = 1/\sqrt{G_{\rm N}} \sim 10^{19}$ GeV. Unless this picture is elusive,[7] it is hard to imagine testing these effects experimentally. Nevertheless, the failure to consistently include gravity in the theory of course strongly suggests that the Standard Model is not the complete story.

Gravity aside, there are astrophysical observations implying directly that physics beyond the Standard Model exists. First, there is the observed baryon asymmetry in the universe (there are only few anti-baryons). To explain this asymmetry, it is believed that $\mathcal{CP}$ violation beyond the CKM framework is required. Second, an important cosmological observation is that $\sim 23\%$ of the total energy content in the universe is in the form of cold dark matter [21]. Should this dark matter consist of elementary particles, they have to be stable over cosmological timescales and interact only weakly with other particles. None of the known particles carry the right properties. A suitable candidate particle for the dark matter is often an important building block when considering theories beyond the Standard Model, not least so in the minimal supersymmetric standard model which will be discussed next.

[7] There might for example be extra dimensions which are responsible for the apparent weakness of the gravitational interaction in 4D. In these theories, the true value of M_P could in fact be as low as $M_P \sim 1$ TeV. In this case, black hole production could be possible at colliders [20].

2. Minimal supersymmetry

> "Omne ignotum pro magnifico est."
>
> Tacitus

As alluded to in the previous chapter, there are issues which cannot be resolved within the Standard Model. Taken together, they call for an extension of the theory around the TeV scale. Appealing to symmetry principles, such as Lorentz and gauge symmetry, has been a successful path for making predictions in the past. A natural continuation along this line is offered by supersymmetry [22]. Supersymmetry (SUSY) provides the unique extension of space-time symmetry to spinorial charges [23], relating fermionic and bosonic degrees of freedom. In this chapter we introduce weak scale supersymmetry, and discuss how it addresses some of the problems in the Standard Model. We then turn to the Higgs sector, before concluding with a discussion of constrained models.

2.1 Concepts of the MSSM

Schematically, a supersymmetry transformation $\mathcal{Q}$ acts on a fermionic state $|F\rangle$ by transforming it into a boson, $\mathcal{Q}|F\rangle = |B\rangle$, and conversely $\mathcal{Q}|B\rangle = |F\rangle$. In this way the minimal supersymmetric standard model (MSSM) [24] doubles the Standard Model particle content. Each chiral fermion q_L is assigned a scalar superpartner $\widetilde{q}_L \leftrightarrow q_L$, resulting in *squarks* $\widetilde{q}$, *sleptons* $\widetilde{\ell}$, and *sneutrinos* $\widetilde{\nu}$. The gauge bosons A_μ acquire fermionic partner *gauginos* $\widetilde{A} \leftrightarrow A_\mu$, leading to the *wino* $\widetilde{W}^\pm$, *zino* $\widetilde{Z}$, *photino* $\widetilde{\gamma}$, and the *gluino* $\widetilde{g}$. Similarly, the fermionic partners $\widetilde{H}$ of the scalar Higgs fields are called *Higgsinos*. The particles related by supersymmetry are grouped together into different supermultiplets, or superfields, for which the allowed interactions are dictated by gauge symmetry and supersymmetry.

The symmetry requires that particles in a common supermultiplet differ only by their spin. In particular this implies that the states should have equal masses. This fact explains immediately how the MSSM can solve the hierarchy problem: for every fermion loop contributing a quadratic divergence $\delta m_h^2 \propto +m_f^2$ to equation (1.35), supersymmetry introduces a scalar contri-

bution $\delta m_h^2 \propto -m_{\tilde{f}}^2$ with opposite sign, and vice versa. Supersymmetry thus protects a light Higgs mass and makes the theory natural. Unfortunately, superpartners with the same masses as the ordinary particles have not been observed experimentally. One must therefore conclude that supersymmetry, if it exists, is broken. Now, breaking supersymmetry explicitly is not difficult; in fact most Lagrangians are *not* supersymmetric. It is however highly desirable to achieve a so-called *soft* breaking, i.e. breaking supersymmetry without regenerating the quadratic divergences. Spontaneous breaking of SUSY in a hidden sector can be mediated to the visible sector at a high scale through different mechanisms. The common result can be presented as an effective theory at the weak scale in which supersymmetry is softly broken. Of all the possible couplings in the effective Lagrangian, only a few correspond to a soft breaking. The soft SUSY-breaking terms have been classified [25] into three simple categories:

$$m_1^2\phi^*\phi + m_2^2\left(\phi^2 + \phi^{*2}\right) \qquad \text{Scalar masses} \qquad (2.1a)$$

$$-\frac{1}{2}M_\lambda\overline{\lambda}\lambda \qquad \text{Gaugino masses} \qquad (2.1b)$$

$$-A\left(\phi^3 + \phi^{*3}\right) \qquad \text{Trilinear A-terms} \qquad (2.1c)$$

In broken supersymmetry, the superpartners receive contributions to their masses both from ordinary Yukawa mass terms and from the soft masses. The soft terms mix states with the same quantum numbers (such as $\widetilde{q}_L$ and $\widetilde{q}_R$). The corresponding mass eigenstates are then obtained by diagonalization. As an example of this, consider the mixing of the neutral EW gauginos[1] with the neutral Higgsinos (there are two of those in the MSSM for reasons which will soon become apparent). The resulting four mass eigenstates $\tilde{\chi}_i^0$ are referred to as *neutralinos*, while the charged counterparts $\tilde{\chi}_i^\pm$ (of which there are two) are called *charginos*.

The proliferation of scalar fields in the MSSM can lead to problems with violation of baryon and lepton number through Yukawa-like couplings which are not present in the SM. This problem can be solved by introducing a discrete symmetry [24] called R-parity. Under this symmetry, fields are given quantum numbers according to

$$R = (-1)^{3B+L+2S}, \qquad (2.2)$$

where B is the baryon number ($+1/3$ for a quark), L the lepton number, and S the spin. It is easy to verify from the definition that ordinary particles have $R = +1$, while superpartners all carry $R = -1$. An exactly conserved R-parity has direct impact on the MSSM phenomenology. It implies that SUSY particles can only be produced in pairs. Furthermore, the lightest supersymmetric particle (LSP) will be stable, which leads to missing energy signatures for

[1] Note that the gluinos do not mix with the EW gauginos due to conservation of colour.

SUSY events at colliders. Another important consequence of R-parity conservation arises when the LSP is electrically neutral, weakly interacting, and has a mass $m \lesssim 1$ TeV. It then makes an excellent candidate for the cold dark matter of the universe. In many scenarios the lightest neutralino $\tilde{\chi}_1^0$ has exactly these properties [26].

2.2 The MSSM Higgs sector

An important consequence of supersymmetry is that the Higgs sector can no longer be of the minimal type introduced in chapter 1. The existence of a single Higgsino fermion would spoil the successful cancellation of the Adler-Bell-Jackiw anomaly in the SM (see e.g. [27]), rendering the theory non-renormalizable. An obvious remedy is to introduce a second Higgs doublet with opposite hypercharge, letting its Higgsino restore the cancellation. There is also a second motivation calling for a second doublet: supersymmetry. In a supersymmetric theory, the superpotential must be written as an analytic function of the fields, i.e. no complex conjugates may appear. This prevents the SM trick played in equation (1.28) to give mass to both up-type and down-type quarks using Φ and Φ^*. Two doublets of opposite hypercharges are again required.[2]

The Higgs potential of the MSSM can be written down directly from a combination of supersymmetric terms and the soft SUSY-breaking terms in equation (2.1a) which involve the Higgs fields. Introducing the two doublets

$$H_d = \begin{pmatrix} H_d^0 \\ H_d^- \end{pmatrix}, \qquad H_u = \begin{pmatrix} H_u^+ \\ H_u^0 \end{pmatrix},$$

with $Y_{H_d} = -1$ and $Y_{H_u} = +1$, the Higgs potential replacing equation (1.21) is given by [28]

$$\begin{aligned} \mathcal{V}_{\text{MSSM}}(H_d, H_u) = {} & m_d^2 |H_d|^2 + m_u^2 |H_u|^2 - B\mu\epsilon_{ab}\left(H_d^a H_u^b + \text{h.c.}\right) \\ & + \frac{g^2 + g'^2}{8}\left(|H_d|^2 - |H_u|^2\right)^2 + \frac{1}{2}g^2 |H_d^\dagger H_u|^2. \end{aligned} \tag{2.3}$$

Here ϵ_{ab} is the completely antisymmetric tensor with $\epsilon_{12} = 1$.[3] The mass parameters are $m_i^2 = m_{H_i}^2 + |\mu|^2$, where $m_{H_i}^2$ are soft masses. For the electroweak symmetry to be broken, both $m_u^2 \neq m_d^2$ and at least one negative mass

[2] One could of course consider supersymmetric models with N Higgs doublets, where $N > 2$ is an even number (again to avoid the ABJ anomaly). By the principle of parsimony, the MSSM has exactly $N = 2$.

[3] The sign of μ is conventional and both choices exist in the literature. This is unfortunate, since the sign is relevant for phenomenology. We adhere to the convention of e.g. the SUSY Les Houches accord [29].

eigenvalue is required. This immediately shows that $m_{H_d}^2 = m_{H_u}^2 = 0$ is not a viable option, i.e. SUSY breaking is a prerequisite for EW symmetry breaking. When the electroweak symmetry is broken, the neutral components of the doublets acquire vacuum expectation values

$$\left\langle H_d^0 \right\rangle \equiv \frac{v_d}{\sqrt{2}} \qquad \left\langle H_u^0 \right\rangle \equiv \frac{v_u}{\sqrt{2}},$$

which can be used to replace m_d^2 and m_u^2 through two minimization conditions. Like in the SM, the overall scale v is fixed by the known gauge boson mass

$$m_Z^2 = \frac{1}{2}\left(g^2 + g'^2\right) v^2 = \frac{1}{2}\left(g^2 + g'^2\right)\left(v_u^2 + v_d^2\right). \tag{2.4}$$

An important role for phenomenology is played by the ratio

$$\tan\beta \equiv \frac{v_u}{v_d}. \tag{2.5}$$

Of the eight degrees of freedom originally present in the two complex doublets, only three correspond to the longitudinal components of $W^\pm$ and Z^0. This leaves five physical Higgs bosons in the spectrum. The real parts of H_d^0 and H_u^0 mix with an angle α to produce two $\mathcal{CP}$-even states h and H (with $m_h < m_H$), while the remaining (imaginary) neutral component is a $\mathcal{CP}$-odd scalar A. Finally, there is a charged Higgs boson pair $H^\pm$. Both the A and $H^\pm$ represent new types of Higgs bosons not present in the SM.

At the minimum, the potential can be described by only two parameters, and the tree-level masses of the Higgs bosons are not independent quantities. Expressed in terms of m_A and $\tan\beta$, the remaining three masses are given by

$$m_{H,h}^2 = \frac{1}{2}\left[m_A^2 + m_Z^2 \pm \sqrt{\left(m_A^2 + m_Z^2\right)^2 - 4 m_A^2 m_Z^2 \cos^2 2\beta}\right] \tag{2.6a}$$

$$m_{H^\pm}^2 = m_A^2 + m_W^2. \tag{2.6b}$$

We also have the mixing angle α in the neutral sector which is determined by the relation

$$\tan 2\alpha = \frac{m_A^2 + m_Z^2}{m_A^2 - m_Z^2} \tan 2\beta. \tag{2.7}$$

Together with $\tan\beta$, this mixing angle determines the couplings of the neutral Higgs bosons to the fermions and gauge bosons. These couplings are given explicitly in chapter 3 for the case of a general two-Higgs-doublet model.

It can be seen directly from equation (2.6a) that the lightest Higgs mass $m_h \leq m_Z$. Such a light Higgs mass is not compatible with the present exper-

imental bounds [30].[4] However, to obtain a more precise prediction for m_h it is necessary to go beyond the tree-level result. Including the most important contribution from the top sector at one loop [31, 32], the correction to m_h is

$$\delta m_h^2 = \frac{3g^2 m_t^4}{8\pi^2 m_W^2}\left[\log\frac{m_{\tilde{t}_1}^2 + m_{\tilde{t}_2}^2}{2m_t^2} + \frac{2X_t^2}{m_{\tilde{t}_1}^2 + m_{\tilde{t}_2}^2}\left(1 - \frac{1}{6}\frac{X_t^2}{m_{\tilde{t}_1}^2 + m_{\tilde{t}_2}^2}\right)\right], \quad (2.8)$$

where $X_t \equiv A_t - \mu\cot\beta$ describes the stop mixing (A_t is the trilinear coupling of stops to H_u). As we can see from this equation, the upper limit on the Higgs mass now depends on the average mass of the stops, as well as on their mixing X_t. When the mixing is large, the correction to m_h can be substantial. Including results from a partial two-loop computation, the tree-level bound is lifted to $m_h \lesssim 135$ GeV [33] for stop parameters of $\mathcal{O}(1$ TeV). In general, the radiatively corrected Higgs sector depends not only on m_A and $\tan\beta$, but on the soft SUSY-breaking parameters as well. Benchmark scenarios have therefore been devised for MSSM Higgs searches [34], taking into account the most relevant parameters. A specific example is the $m_h^{\max}$ scenario, which maximizes m_h for a given value of $\tan\beta$, leading to conservative exclusion bounds. From equation (2.8) we see that maximizing m_h at one loop corresponds to $X_t = \pm\sqrt{6}M$, where M is the average stop mass.[5] To summarize this section we stress that, even with radiative corrections included, the MSSM definitely predicts at least one *light* Higgs boson in line with the preference of the electroweak precision data. It is therefore a reasonable conclusion that this Higgs boson is within the discovery reach of the LHC, should the MSSM be the correct theory of nature.

2.3 Unification and constrained MSSM

The softly broken MSSM with R-parity conservation has 124 parameters, of which 19 are present in the Standard Model and 105 are new. Working with a model that has this many free parameters is not practical. Furthermore, many of the parameters in the general MSSM generate phenomenologically unacceptable effects, such as tree-level flavour-changing neutral currents (FCNC), non-conservation of the individual lepton numbers L_e, L_μ, and L_τ, or large electric dipole moments of e.g. the neutron. To address these issues, one can make the additional assumptions:

1. All soft SUSY-breaking parameters are real. This forbids any new source of $\mathcal{CP}$ violation.

[4] Certain exceptions exist also within the MSSM. Scenarios with non-zero $\mathcal{CP}$ phases in the Higgs sector can for instance have $m_h \leq 15$ GeV without conflicting experiment.

[5] Going to the two-loop calculation, the value for X_t which maximizes m_h depends on the renormalization scheme. The relation $X_t = \sqrt{6}M$ holds in the $\overline{\text{MS}}$ scheme [32].

2. The sfermion mass matrices and the trilinear couplings are diagonal in the same flavour basis as the fermion masses. This eliminates tree-level FCNCs.

These assumptions remove ~ 70 mixing angles and phases from the MSSM parameter set and improve drastically the odds of obtaining a phenomenologically viable model.

So far this discussion concerned a purely phenomenological way of restricting the number of MSSM parameters. The same reduction can be achieved more elegantly in a top-down approach. This idea stems from the observation [35] that the MSSM with sparticle masses around 1 TeV allows for gauge coupling unification at a scale $M_{\text{GUT}} \simeq 10^{16}$ GeV. In a unified model, SUSY breaking is assumed to be mediated in such a way that only a few universal parameters describe the theory at the GUT scale. Starting from this relatively small number of parameters, the soft breaking and weak scale parameters are obtained through renormalization group running. Non-universalities in the weak scale parameters develop through their different renormalization. One important consequence of the running is that a Higgs potential starting with universal Higgs mass parameters $m^2_{H_d} = m^2_{H_u}$ at the GUT scale can develop $m^2_{H_d} \neq m^2_{H_u} < 0$ at the EW scale, which triggers the electroweak symmetry breaking. This phenomenon is called radiative electroweak symmetry breaking.

The minimal top-down model in widespread use is inspired by gravity-mediated SUSY breaking. It is called the constrained MSSM (CMSSM),[6] and contains only four parameters (and a sign) in addition to those of the standard model:

m_0	the universal scalar mass,
$m_{1/2}$	the universal gaugino mass,
A_0	the universal trilinear coupling,
$\tan\beta$	the ratio v_u/v_d of the vacuum expectation values,
$\text{sign}(\mu)$	the sign of the Higgsino mass parameter.

All the parameters, except $\tan\beta$, are specified at the unification scale. The value of $|\mu|$ is *not* a free parameter, but it is determined by the condition for electroweak symmetry breaking

$$|\mu|^2 = \frac{m^2_{H_d} - m^2_{H_u}\tan^2\beta}{\tan^2\beta - 1} - \frac{1}{2}m_Z^2. \tag{2.9}$$

[6]The CMSSM is also commonly referred to as minimal supergravity (mSUGRA), although mSUGRA models should require the additional relations $m^2_{3/2} = m_0^2$ and $B_0 = A_0 - m_{3/2}$ for the gravitino mass $m_{3/2}$ and the bilinear coupling B_0 at the GUT scale [36]. In mSUGRA $\tan\beta$ is not a free parameter, but it can be determined from the EWSB conditions [37].

As variations of the CMSSM, models in which the Higgs mass parameters m_{H_d} and m_{H_u} do not unify with the other scalar masses have been introduced [38]. This class of models goes by the name of non-universal Higgs mass models (NUHM). One introduces either a single new GUT-scale parameter: $m_{H_d} = m_{H_u} \neq m_0$, or treat both m_{H_d} and m_{H_u} at the high scale as free parameters. In the second case with two parameters, equation (2.9) and the weak scale relation

$$m_A^2 = m_{H_d}^2 + m_{H_u}^2 + 2|\mu|^2 \tag{2.10}$$

may be used as boundary conditions to replace the GUT-scale Higgs mass parameters by the values of $|\mu|$ and m_A as input at the EW scale. Since m_A and $\tan\beta$ completely determine the Higgs sector at tree-level, NUHM provides an interesting starting point for Higgs phenomenology in the MSSM. In papers I and II we discuss flavour physics constraints and prospects for charged Higgs boson searches at the LHC in the CMSSM and NUHM frameworks.

3. General two-Higgs-doublet models

In the previous chapter we have seen a specific example of a model with two Higgs doublets – a two-Higgs-doublet model (2HDM) – in the form of the MSSM Higgs sector. We now widen the discussion to more general two-Higgs-doublet models [39]. In a bottom-up approach, adding an extra doublet can be considered a minimal extension of the SM Higgs sector. Most of what is discussed in this chapter has been implemented in the computer code `2HDMC`, which enables phenomenological studies of general two-Higgs-doublet models.[1] The code itself is described in more detail in paper III.

3.1 The 2HDM Higgs potential

To connect to the literature on general two-Higgs-doublet models [28], we start from two complex scalar SU(2) doublets, Φ_1 and Φ_2. Both doublets are taken to have hypercharge $Y = +1$, which is different from the MSSM case. The two doublets are related by a unitary transformation, $\Phi_a \to \Phi'_a = U_{ab}\Phi_b$. Requiring a Higgs potential which is gauge invariant, renormalizable, and invariant under U(2) transformations, the most general expression is [40]

$$\begin{aligned}\mathcal{V}_{\text{2HDM}} = {} & m_{11}^2 \Phi_1^\dagger \Phi_1 + m_{22}^2 \Phi_2^\dagger \Phi_2 - \Big[m_{12}^2 \Phi_1^\dagger \Phi_2 + \text{h.c.} \Big] + \frac{1}{2}\lambda_1 \left(\Phi_1^\dagger \Phi_1 \right)^2 \\ & + \frac{1}{2}\lambda_2 \left(\Phi_2^\dagger \Phi_2 \right)^2 + \lambda_3 \left(\Phi_1^\dagger \Phi_1 \right) \left(\Phi_2^\dagger \Phi_2 \right) + \lambda_4 \left(\Phi_1^\dagger \Phi_2 \right) \left(\Phi_2^\dagger \Phi_1 \right) \\ & + \left\{ \frac{1}{2}\lambda_5 \left(\Phi_1^\dagger \Phi_2 \right)^2 + \Big[\lambda_6 \left(\Phi_1^\dagger \Phi_1 \right) + \lambda_7 \left(\Phi_2^\dagger \Phi_2 \right) \Big] \left(\Phi_1^\dagger \Phi_2 \right) + \text{h.c.} \right\}. \end{aligned} \tag{3.1}$$

This potential contains 14 parameters in total, since m_{12}^2 and λ_{5-7} can be complex valued, while the remaining parameters m_{11}^2, m_{22}^2, and λ_{1-4} are real (since $\mathcal{V}$ is real). Complex phases in the potential which cannot be removed by a basis transformation on the Higgs fields lead to violation of $\mathcal{CP}$. In a $\mathcal{CP}$-conserving model, all parameters can be taken as real numbers. The total (maximum) number of free parameters then becomes ten. Comparing $\mathcal{V}_{\text{2HDM}}$ to the MSSM Higgs potential given by equation (2.3), the quartic couplings are related in the following way: $\lambda_1 = \lambda_2 = (g^2 + g'^2)/4$, $\lambda_3 = (g^2 - g'^2)/4$, $\lambda_4 = -g^2/2$, and $\lambda_{5-7} = 0$. Since the gauge couplings are real, $\mathcal{CP}$ is con-

[1] The `2HDMC` code is publicly available at `http://www.isv.uu.se/thep/MC/2HDMC`.

Coupling	h	H	A
$H_i W^+ W^-$	$\sin(\beta-\alpha)$	$\cos(\beta-\alpha)$	0
$H_i Z Z$	$\sin(\beta-\alpha)$	$\cos(\beta-\alpha)$	0
$H_i Z A$	$\cos(\beta-\alpha)$	$\sin(\beta-\alpha)$	0
$H_i W^\pm H^\mp$	$\cos(\beta-\alpha)$	$\sin(\beta-\alpha)$	1
$H_i Z W^\pm H^\mp$	$\cos(\beta-\alpha)$	$\sin(\beta-\alpha)$	1
$H_i \gamma W^\pm H^\mp$	$\cos(\beta-\alpha)$	$\sin(\beta-\alpha)$	1

Table 3.1: *Dependence on the mixing angle $\beta-\alpha$ for the couplings of Higgs bosons to gauge bosons in the $\mathcal{CP}$-conserving 2HDM.*

served at tree-level. The general form (3.1) of the 2HDM potential provides the effective description of the MSSM Higgs potential when radiative corrections are taken into account [41], or when higher-dimensional operators are included at tree-level to describe physics beyond the MSSM [42].

We will not go through the details of electroweak symmetry breaking in the general 2HDM, since it mostly follows the discussion in section 2.2. Staying with a $\mathcal{CP}$-conserving model, eliminating two parameters at the minimum in favour of the vacuum expectation values, we are left with the parameters

$$\left\{\lambda_1,\, \lambda_2,\, \lambda_3,\, \lambda_4,\, \lambda_5,\, \lambda_6,\, \lambda_7,\, m_{12}^2\right\}, \tag{3.2}$$

and $\tan\beta$ which specifies a basis in the Higgs field space. Since invariance under a redefinition of the Higgs fields has been a guiding principle when constructing the potential, there is nothing which distinguishes Φ_1 from Φ_2. One may of course choose to work in a basis where $\langle\Phi_1\rangle = v_1/\sqrt{2} = v\cos\beta/\sqrt{2}$, $\langle\Phi_2\rangle = v_2/\sqrt{2} = v\sin\beta/\sqrt{2}$ (similarly to the MSSM), but it should then be remembered that $\tan\beta$ at this stage is not a physical parameter, hence its value is arbitrary. Working at tree-level, it is sometimes convenient to replace the parameters of equation (3.2) by the set

$$\left\{m_h,\, m_H,\, m_A,\, m_{H^\pm},\, \sin(\beta-\alpha),\, \lambda_6,\, \lambda_7,\, m_{12}^2\right\}. \tag{3.3}$$

The mixing $s_{\beta-\alpha} \equiv \sin(\beta-\alpha)$ and $c_{\beta-\alpha} \equiv \cos(\beta-\alpha)$ determines the couplings of Higgs bosons to gauge bosons in a pattern which can be seen in table 3.1. Two additional couplings, which are both independent of $s_{\beta-\alpha}$, are ZH^+H^- and γH^+H^-. It should also be mentioned that there are no $\gamma H^\pm W^\mp$ or $ZH^\pm W^\pm$ vertices in the 2HDM. The remaining parameters λ_6, λ_7, and m_{12}^2 could be related to quartic Higgs self-couplings which (at least in principle) are measurable quantities.

Even in the absence of supersymmetry there are ways in which a physically relevant basis can be specified for the Higgs fields. Introducing an ad-hoc Z_2

symmetry under which

$$\begin{aligned} \Phi_1 &\to \Phi_1 \\ \Phi_2 &\to -\Phi_2 \end{aligned} \tag{3.4}$$

(or vice versa), it becomes possible to distinguish between the doublets. As can be seen from equation (3.1), the terms proportional to λ_6, λ_7, and m_{12}^2 violate this symmetry; non-zero λ_6 and λ_7 correspond to a hard Z_2 violation, whereas the dimension two m_{12}^2 term leads to a soft violation [43]. In section 3.2 we demonstrate how $\tan\beta$ is given a physical meaning in the case of a 2HDM with a Z_2 symmetry.

3.2 The Yukawa sector

In this discussion of the 2HDM Yukawa sector, we follow the conventions of [44]. For simplicity, we assume that the Yukawa interactions admit no complex phases beyond the single one present in the CKM matrix. For an extended treatment, including $\mathcal{CP}$ violation, we refer to [45].

The generalization of the SM Yukawa couplings, equation (1.30), to the case of two Higgs doublets is straightforward:

$$\begin{aligned} -\mathcal{L}_{\text{Yukawa}} =& \overline{Q}_L \left(Y_1^D \Phi_1 + Y_2^D \Phi_2\right) D_R + \overline{Q}_L \left(Y_1^U \widetilde{\Phi}_1 + Y_2^U \widetilde{\Phi}_2\right) U_R \\ &+ \overline{L}_L \left(Y_1^L \Phi_1 + Y_2^L \Phi_2\right) E_R + \text{h.c.} \end{aligned} \tag{3.5}$$

The Yukawa couplings Y_1^F and Y_2^F ($F = D, U, L$) are 3×3 matrices in flavour space. Working in an arbitrary basis where $v_1 = v\cos\beta$, $v_2 = v\sin\beta$, one can introduce the linear combinations

$$\begin{cases} \kappa_0^F = Y_1^F \cos\beta + Y_2^F \sin\beta \\ \rho_0^F = -Y_1^F \sin\beta + Y_2^F \cos\beta. \end{cases} \tag{3.6}$$

Replacing the doublets by their vacuum expectation values in equation (3.5), the terms proportional to κ_0^F couple to v, while the terms proportional to ρ_0^F vanish. Performing unitary transformations on the fermion fields, it is in general possible to transform the linear combination corresponding to the mass matrix into the diagonal form

$$M^F = \frac{v}{\sqrt{2}}\kappa^F = \frac{v}{\sqrt{2}} \left(V_L^F\right)^\dagger \kappa_0^F V_R^F . \tag{3.7}$$

The orthogonal combination ρ_0^F is diagonalized[2] simultaneously with κ_0^F only under special conditions. An elegant way to ensure this property was pro-

[2]Technically speaking, equation (3.7) is a singular value decomposition of κ_0^F, but we are sloppy and use the term diagonalization unless there is a risk for confusion.

posed by Glashow and Weinberg [46], who showed that a sufficient criterion is that all right-handed fermions of a given electric charge couple only to one Higgs doublet. This can be achieved using the Z_2 symmetry introduced above. Choosing transformation rules for the right-handed fermions under the same symmetry, some of the couplings in equation (3.5) are forbidden. For fermions that couple only to Φ_1, equation (3.6) gives the relation $\rho_0^F = -\tan\beta\kappa_0^F$, while a coupling to Φ_2 corresponds to $\rho_0^F = \cot\beta\kappa_0^F$. A simultaneous diagonalization of ρ^0 and κ^0 is possible in this case since the matrices are proportional. The MSSM couplings – called the 2HDM type II – are obtained by coupling Φ_2 to the up-type quarks, and Φ_1 to the down-type quarks and leptons. In a type I model, all fermions instead couple to the same doublet, while the second doublet has no fermion couplings at all. As discussed in paper IV, there exist even more options for how to arrange the 2HDM Yukawa sector.

Expanding the doublets in the physical (mass) eigenstates, the Lagrangian describing the couplings of the neutral Higgs bosons to fermions are given by

$$-\mathcal{L}_{\mathrm{Y}} = \frac{1}{\sqrt{2}}\overline{F}\Big[\kappa^F\left(hs_{\beta-\alpha} + Hc_{\beta-\alpha}\right) + \rho^F\left(hc_{\beta-\alpha} - Hs_{\beta-\alpha} \pm \mathrm{i}\gamma^5 A\right)\Big]F, \tag{3.8}$$

where F (either U, D, or L) is a vector in flavour space. The sign of the last term in equation (3.8) is negative for $F = U$, otherwise positive. As we can see from this equation, off-diagonal elements in ρ^F generate FCNCs at tree-level, something which is severely constrained by experiment. Returning to the special case of the 2HDM type II (the MSSM at tree-level), Feynman rules for the vertices read explicitly

$$\begin{aligned}
h\overline{u}u\colon &\quad -\mathrm{i}\frac{m_u}{v}\frac{\cos\alpha}{\sin\beta}, & H\overline{u}u\colon &\quad -\mathrm{i}\frac{m_u}{v}\frac{\sin\alpha}{\sin\beta}, & A\overline{u}u\colon &\quad -\frac{m_u}{v}\cot\beta\,\gamma^5,\\
h\overline{d}d\colon &\quad \mathrm{i}\frac{m_d}{v}\frac{\sin\alpha}{\cos\beta}, & H\overline{d}d\colon &\quad -\mathrm{i}\frac{m_d}{v}\frac{\cos\alpha}{\cos\beta}, & A\overline{d}d\colon &\quad -\frac{m_d}{v}\tan\beta\,\gamma^5.
\end{aligned} \tag{3.9}$$

Here m_u and m_d denote masses of arbitrary up- and down-type quarks. The couplings for leptons in the 2HDM type II follow the pattern for the down-type quarks. These couplings illustrate that $\tan\beta$ is promoted to a physical parameter through its role in the Yukawa couplings of the Z_2-symmetric models. The specific value of $\tan\beta$ where the symmetry is implemented is singled out. For the couplings of the charged Higgs boson, we have

$$-\mathcal{L}_{\mathrm{Y}} = \overline{U}\big(V_{\mathrm{CKM}}\rho^D P_R - \rho^U V_{\mathrm{CKM}}^* P_L\big)DH^+ + \overline{\nu}\rho^L P_R L H^+ + \mathrm{h.c.}, \tag{3.10}$$

which for the 2HDM type II translates into the rules (all particles going into the vertex)

$$\begin{aligned}
H^+\overline{u}d\colon &\quad \frac{\mathrm{i}}{\sqrt{2}v}V_{ud}\left[m_d\tan\beta\,(1+\gamma^5) + m_u\cot\beta\,(1-\gamma^5)\right],\\
H^-\overline{d}u\colon &\quad \frac{\mathrm{i}}{\sqrt{2}v}V_{ud}\left[m_d\tan\beta\,(1-\gamma^5) + m_u\cot\beta\,(1+\gamma^5)\right].
\end{aligned} \tag{3.11}$$

4. High-energy $H^{\pm}$ phenomenology

In this chapter we describe the phenomenology of charged Higgs bosons at colliders, focusing primarily on the MSSM. We begin with a concise general introduction to the implementation of hadron collider physics in a Monte Carlo generator. We then proceed to discuss the main production and decay modes of $H^{\pm}$ at the Large Hadron Collider. This chapter provides background for the work presented in papers I, II, VI, and VII.

4.1 QCD for hadron colliders

In section 1.2 we discussed that the QCD partons are confined into hadrons. As a consequence of this fact, a realistic description of the physics in a high-energy pp or $p\bar{p}$ collision requires several steps of calculation and modelling. Monte Carlo event generators are indispensable tools for simulating the complex scattering events in a way reminiscent of the experimental reality. We therefore give a general overview of the physics ingredients necessary for a Monte Carlo study of any process in a hadronic collision.

The hard scattering

The parton-level (hard) matrix element $\mathcal{M}$ of the process we are interested in is computed from the Feynman rules of the theory. From the matrix element, the differential cross section for $2 \to n$ scattering

$$\mathrm{d}\hat{\sigma}_{ij\to n} = \frac{1}{2\hat{s}}|\mathcal{M}|^2 \mathrm{d}\Phi_n \tag{4.1}$$

is obtained, where $\mathrm{d}\Phi_n$ denotes the n-body phase space and $\hat{s} = (p_i + p_j)^2$. Historically most generators have used simple $2 \to 2$ or $2 \to 3$ matrix elements, but today's automatized techniques have made the use of tree-level matrix elements with high multiplicities feasible.[1] There has also been a considerable development in the implementation of full NLO matrix elements [47] in event generators. Using QCD factorization, the hadron-level cross sec-

[1] There are too many matrix element generators on the market to list them all here. The web site `http://www.ippp.dur.ac.uk/montecarlo/BSM/` maintains an (incomplete) list of tools for physics beyond the Standard Model.

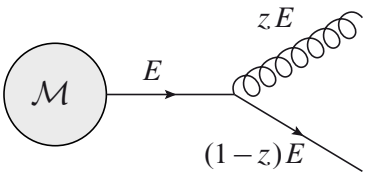

Figure 4.1: Kinematics in the branching of a final state parton $q \to qg$.

tion

$$\mathrm{d}\sigma_{pp\to n} = \sum_{i,j} \int \mathrm{d}x_1 \mathrm{d}x_2 f_i\left(x_1, \mu_\mathrm{F}^2\right) f_j\left(x_2, \mu_\mathrm{F}^2\right) \mathrm{d}\hat{\sigma}_{ij\to n}\left(x_1, x_2, \mu_\mathrm{F}^2, \mu_\mathrm{R}^2, s\right), \tag{4.2}$$

is computed from the hard cross section by folding with the parton distribution functions $f(x, \mu_\mathrm{F}^2)$ of the proton.

Parton showers

In a way similar to the DGLAP evolution of the parton distributions, perturbative QCD can also be used to describe the occurrence of real radiation from coloured particles present in the initial and final states of a hard collision. Since the matrix elements for radiating extra partons are singular in the soft and collinear limits, radiation will be abundant in those regions of phase-space. The process of generating successive emissions can be described iteratively in a *parton shower*. In the collinear limit, the differential probability that a branching occurs at a scale Q^2, with one of the resulting partons carrying a fraction z of the original parton's energy (see figure 4.1), is

$$\mathrm{d}\mathcal{P}_{i\to jk} = \frac{\alpha_s}{2\pi} \sum_{j,k} \frac{\mathrm{d}Q^2}{Q^2} P_{i\to jk}(z)\mathrm{d}z. \tag{4.3}$$

$P_{i\to jk}$ are the splitting functions. For a final state shower, starting the evolution at the hard scale $Q_\mathrm{max}^2 \sim \hat{s}$, the next scale Q_1^2 at which a branching occurs is obtained by multiplying the differential probability of equation (4.3) with the *Sudakov form factor*

$$\Delta_i\left(Q_1^2, Q_\mathrm{max}^2\right) = \exp\left[-\sum_{j,k} \int_{Q_1^2}^{Q_\mathrm{max}^2} \frac{\mathrm{d}Q^2}{Q^2} \int \frac{\alpha_s}{2\pi} P_{i\to jk}(z)\mathrm{d}z\right], \tag{4.4}$$

which corresponds to the probability that *no* splitting occurred for $Q^2 > Q_1^2$. For the initial state (space-like) parton shower, a backwards evolution from the hard scale is performed using a modified form factor [48], which then also depends on the parton distributions.

Applying a parton shower evolution to all partons from the hard matrix element dresses up the event with radiation to describe the observed jet structure of high-energy scattering events. However, the parton shower approach is strictly speaking valid only in the collinear approximation. The emission of additional jets with high p_T is often better described using a higher order matrix element. Methods have therefore been devised for how to match high-multiplicity matrix elements to a parton shower without double-counting [49].

Hadronization

At the end of the final state parton shower, the partons have evolved from the hard scale down to a scale $Q_0^2 \sim 1$ GeV^2. This is the energy regime where perturbative calculations become questionable, and the QCD partons get confined into colour-neutral hadrons by a process known as *hadronization*. This process is not understood from first principles, and to obtain a description of the hadronic final state requires modelling. An advantage of using the parton shower approach is that it allows for a smooth transition between the partonic final state and a non-perturbative hadronization model at low Q^2.

There are two dominating approaches to hadronization. One is the Lund string model [50], which is used in `PYTHIA` [51] and several other Monte Carlo codes from the same 'family'. In the string model, a string-like energy configuration is stretched between the outgoing partons of a colour-connected $q\bar{q}$ pair. Intermediate gluons are treated as kinks on these triplet strings. The strings are then fragmented iteratively into hadrons by the creation of new $q\bar{q}$ pairs in the colour field. The second model in widespread use is the cluster model, implemented in the `HERWIG` Monte Carlo [52]. In this model, gluons first undergo a forced splitting into $q\bar{q}$ pairs. Neighbouring colour triplets are then connected from the colour structure of the cascade, forming singlet *clusters* which subsequently are decayed into hadrons. Both models describe collider data successfully. Following the hadronization, any unstable hadrons created are allowed to decay further into the particles observed in detectors.

The underlying event

In addition to the steps discussed, the modelling of a hadronic collision requires some treatment of the beam remnants. Data also indicates that more than two partons on average undergo hard scattering for each pp collision. Each of these collisions in turn generate its own radiation, and there could possibly be non-perturbative cross-talk between different parts of the event. Everything not directly related to the hard scattering is commonly referred to as the *underlying event*. To properly describe the underlying event requires a mixture of perturbative and non-perturbative modelling. Validating the underlying event models for LHC physics will be important to correctly describe backgrounds to new physics searches.

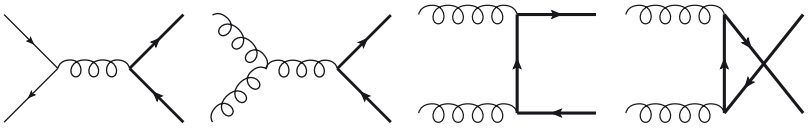

Figure 4.2: Leading order diagrams for $t\bar{t}$ production. Heavy lines indicate top quarks.

4.2 Charged Higgs production

The dominating production mode for a charged Higgs boson at a hadron collider depends, of course, both on the model and the kinematics. For the model, we generally assume MSSM couplings. According to equation (3.11), the charged Higgs couplings in the MSSM are proportional to the fermion masses. Hence the production is dominated by processes involving t and b quarks. By convention, a kinematic division is made into two distinct regions: the *light* $H^\pm$ ($m_{H^\pm} < m_t - m_b$), and the *heavy* $H^\pm$ ($m_{H^\pm} > m_t - m_b$).

When the charged Higgs boson is light, it can be produced from the decay of on-shell top quarks. In the narrow width approximation, the inclusive cross section is given by the factorized expression

$$\sigma_{pp\to\bar{t}bH^+} = \sigma_{pp\to t\bar{t}} \times \mathrm{BR}(t \to bH^+). \tag{4.5}$$

The first factor corresponds to hadroproduction of $t\bar{t}$, which we assume can be completely described within the SM (see [53] for a review of top physics). The leading order diagrams contributing to this process are shown in figure 4.2. At present, the total cross section is known to complete NLO, with many improvements existing in terms of approximate NNLO and soft gluon resummations. For $m_t = 171$ GeV, using CTEQ6.5 parton distributions, the cross section amounts to $\sigma_{pp\to t\bar{t}} \simeq 908$ pb at the LHC ($\sqrt{s} = 14$ TeV), while at the Tevatron ($\sqrt{s} = 1.96$ TeV) the corresponding number is $\sigma_{p\overline{p}\to t\bar{t}} \simeq 7.6$ pb [54]. The combined uncertainties from scale variations and the parton distributions are of order 10% in these numbers. At both energies the cross section is large enough for the production of light charged Higgs bosons to be experimentally relevant. At the LHC, the experimental situation for top physics will improve drastically, going from the few thousands of top quarks produced in total at the Tevatron to literally millions per year.[2] An interesting aspect of $t\bar{t}$ production, which then becomes accessible to measurement, is the presence of spin correlations [55]. Since $\Gamma_t \gg \Lambda_{\mathrm{QCD}}$, the top quark decays before it hadronizes, transferring these correlations to its decay products. In papers VI and VII we have investigated how the SM predictions for this process are affected by the presence of the $t \to bH^+$ decay, and how the spin correlations can be used to gain more information about the charged Higgs couplings.

[2]For the LHC running at *low* luminosity, corresponding to $\int \mathcal{L} \sim 10$ fb^{-1} per year, we expect of order 10^7 $t\bar{t}$ pairs to be produced annually.

In the Standard Model, the decay of the top quark is completely dominated by $t \to bW^+$, accounting for an approximate fraction $|V_{tb}|^2/\left(|V_{td}|^2+|V_{ts}|^2+|V_{tb}|^2\right) = 99.8\%$ of all top decays. For the decay into a charged Higgs boson, the tree-level partial width is given by

$$\begin{aligned}\Gamma^{\text{tree}}_{t\to bH^+} =& \frac{g^2}{64\pi m_W^2}|V_{tb}|^2 m_t \lambda^{1/2}(1,q_{H^+},q_b)\times \\ & \left[(1-q_{H^+}+q_b)\left(m_t^2\cot^2\beta + m_b^2\tan^2\beta\right)+4m_b^2\right],\end{aligned} \tag{4.6}$$

where $q_i = m_i^2/m_t^2$ and $\lambda(1,x,y) = 1+x^2+y^2-2(x+y+xy)$ is the Källén function. This width has a minimum for $\tan\beta = \sqrt{m_t/m_b} \simeq 7$. For small values of $m_{H^\pm}$,[3] and either large or small $\tan\beta$, $\Gamma_{t\to bH^+}$ may become comparable to $\Gamma_{t\to bW^+}$. There are several ways in which the tree-level expression can be improved. The finite $\mathcal{O}(\alpha_s)$ corrections are known [58], as is the procedure for handling the leading logarithmic corrections $\alpha_s^n \log^n(m_t/m_b)$ [59]. They are resummed to all orders by using the running b quark mass $\overline{m}_b\left(m_t^2\right)$ in the coupling.

In the MSSM, there are additional corrections to equation (4.6) which can be crucial for a reliable prediction. The most important corrections result from non-holomorphic Higgs couplings, i.e. induced Yukawa couplings of fermions to the 'wrong' Higgs doublet. Since the effects of interest are numerically largest for the b quark coupling at high $\tan\beta$, we will use this case to illustrate the principle, neglecting for the moment all other fermions. Starting from the Yukawa couplings, the only term allowed in the MSSM at tree-level is

$$-\mathcal{L} = y_b \epsilon_{ij} \overline{q}_L^i H_d^j b_R + \text{h.c.}$$

Quantum corrections to this expression generated through loop effects [60] may be written generically as

$$-\mathcal{L} = (y_b+\delta y_b)\epsilon_{ij}\overline{q}_L^i H_d^j b_R + \Delta y_b \overline{q}_L^i H_u^{i*} b_R + \text{h.c.} \tag{4.7}$$

The non-holomorphic correction Δy_b involves H_u^*, which signals broken supersymmetry since this term is forbidden in the supersymmetric theory. Expressions for δy_b and Δy_b in terms of the MSSM parameters can be found in [33] (and references therein). We can now use equation (3.6) to determine

$$\kappa_b = y_b \cos\beta\left(1+\frac{\delta y_b}{y_b}+\tan\beta\frac{\Delta y_b}{y_b}\right) \tag{4.8a}$$

$$\rho_b = -y_b \sin\beta\left(1+\frac{\delta y_b}{y_b}-\cot\beta\frac{\Delta y_b}{y_b}\right), \tag{4.8b}$$

[3] We will not consider the case $m_{H^\pm} < m_W$ at all, since this is experimentally disfavoured by direct searches [56, 57]. As we show in paper I, the indirect lower limit on $m_{H^\pm}$ is stronger in many MSSM scenarios.

Keeping only the term enhanced by $\tan\beta$, the relation between m_b and the Yukawa coupling y_b gets modified, corresponding to the replacement

$$\frac{m_b}{v} \to \frac{1}{1+(\Delta y_b/y_b)\tan\beta}\frac{m_b}{v} \tag{4.9}$$

in equations (3.9) and (3.11). For typical MSSM scenarios, the corrections may reach $\Delta y_b/y_b \sim 10^{-2}$ (and can be of either sign), which for $\tan\beta \gtrsim 50$ amounts to a sizable correction. As a final point on the non-holomorphic corrections, we emphasize the different notations $\frac{\Delta y_b}{y_b}\tan\beta = \epsilon_b \tan\beta = \Delta m_b = \Delta_b$, which are all in use.

After this short detour, we can now apply the non-holomorphic corrections to the $t \to bH^+$ width at high $\tan\beta$. Incorporating at the same time the resummed QCD corrections, the final expression [61] for the improved width in the $q_b \to 0$ limit becomes

$$\begin{aligned}\Gamma^{\rm MSSM}_{t\to bH+} =& \frac{g^2}{64\pi m_W^2}|V_{tb}|^2 m_t (1-q_{H+})^2 \frac{\overline{m}_b^2(m_t^2)}{(1+\epsilon_b\tan\beta)^2}\tan^2\beta \\ &\times\left\{1+\frac{\alpha_s}{\pi}\left[7-\frac{8\pi^2}{9}-2\log(1-q_{H+})+2(1-q_{H+})\right.\right. \\ &\left.\left.+\left(\frac{4}{9}+\frac{2}{3}\log(1-q_{H+})\right)(1-q_{H+})^2\right]\right\}.\end{aligned} \tag{4.10}$$

A numerical comparison of the leading order decay width, given by equation (4.6), to the full expression (4.10) is shown in figure 4.3 for two different values of $\tan\beta$. The MSSM corrections correspond to the $m_h^{\rm max}$ scenario [34] (with a positive value for the μ parameter).

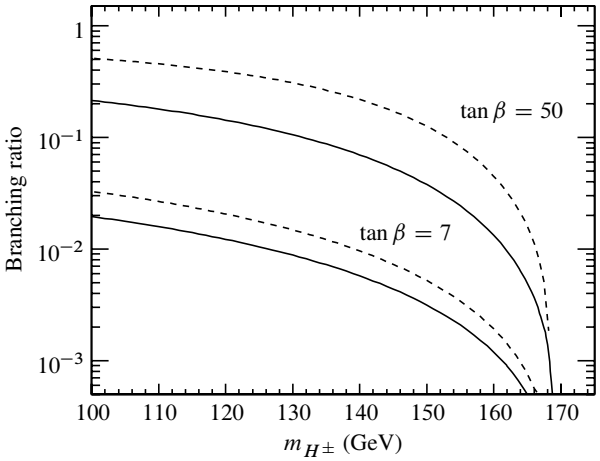

Figure 4.3: Branching ratio for the decay $t \to bH^+$ calculated at tree-level (dashed lines), and using the RGE-improved NLO expression in the $m_h^{\rm max}$ scenario (solid).

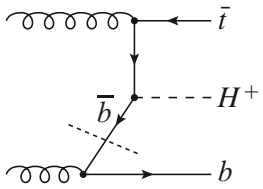

Figure 4.4: Tree-level diagram for the production of a heavy charged Higgs boson in association with a top quark. The dotted line indicates the separation between $gg \to \bar{t}bH^+$, with a hard b quark, and $\bar{b}g \to \bar{t}H^+$ in the collinear limit.

When the charged Higgs is heavy ($m_{H^\pm} > m_t - m_b$), it is not produced on-shell in the decay of any SM particle. The dominant mode of production at the LHC is instead presumed to be in association with a top quark through the parton-level process

$$gg \to tbH^\pm, \tag{4.11}$$

for which a diagram is shown in figure 4.4. The calculation of $\sigma_{pp\to tbH^\pm}$ can proceed in two different ways: when the b quark receives a substantial p_T, the kinematics is correctly described by the process (4.11). On the other hand, in the limit where the b becomes collinear with the incoming gluon, a better description is given by considering $bg \to tH^\pm$, treating the initial state b quark as a massless parton (the five-flavour scheme). The two approaches need to be properly matched to avoid double-counting [62]. Matching of the differential cross section to a parton shower Monte Carlo was performed in [63]. Beyond leading order, $gg \to tbH^\pm$ is part of the real NLO corrections to $gb \to tH^\pm$. The full NLO calculation has been performed both in the five-flavour scheme [64, 65], and more recently in a four-flavour scheme [66]. The corrections increase the total cross section by order 30% compared to the tree-level result, and the scale dependence is significantly reduced. In the same manner as for the decay $t \to bH^+$ discussed above, the most important SUSY corrections to this process come from the non-holomorphic Yukawa corrections at high $\tan\beta$. They are included by performing the replacement according to equation (4.9) in the charged Higgs coupling. Figure 4.5 shows the total LHC cross section $\sigma_{pp\to t\bar{b}H^-}$ [65] as a function of $m_{H^\pm}$ for different values of $\tan\beta$. The shaded areas in the figure indicate the variation of the cross section when varying ϵ_b in the range $-0.01 < \epsilon_b < 0.01$. The cross section for producing a heavy charged Higgs boson is too low in the MSSM to be of interest at the Tevatron.

Besides the dominant QCD production discussed here, alternative modes can be important in special cases. One process which is potentially interesting for high $\tan\beta$ in the intermediate $m_{H^\pm}$ range is the associated production $b\bar{b} \to H^\pm W^\mp$. Other examples include charged Higgs pair production $q\bar{q}(gg) \to H^\pm H^\mp$, or the associated production of the charged and $\mathcal{CP}$-odd

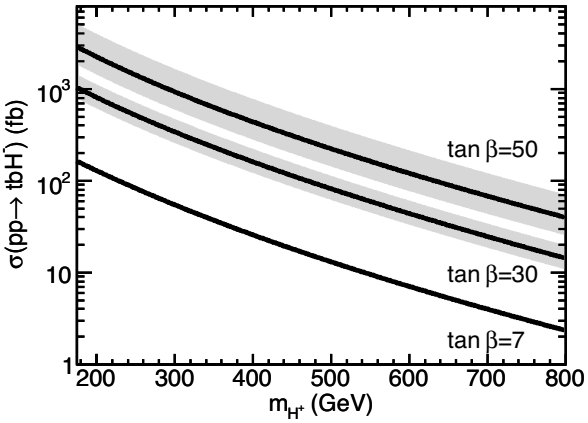

Figure 4.5: Cross section at NLO for production of heavy charged Higgs bosons at the LHC [65]. To include the charge conjugate mode the cross section should be multiplied by two. Bands indicate variations due to SUSY corrections for $|\epsilon_b| < 10^{-2}$.

Higgs bosons through $q\overline{q}' \to H^{\pm}A$. The cross sections for the last two modes are independent of $\tan\beta$, making them particularly suitable for establishing model-independent limits on $m_{H^{\pm}}$. However, since the production proceeds through the weak interaction, the cross sections are significantly lower than for the QCD-initiated production at high $\tan\beta$. At the LHC they can therefore only be interesting for low $m_{H^{\pm}}$.

4.3 Charged Higgs decay

In the MSSM, the charged Higgs boson decays preferentially into the heaviest pair of fermions kinematically accessible, depending on $\tan\beta$ and subject to CKM suppression. This is quite unlike the decay of the weak gauge bosons, which are more 'democratic' in the distribution over different fermionic states. The decay width of $H^{\pm}$ to a pair of fermions is given by

$$\begin{aligned}\Gamma^{\text{tree}}_{H^+\to u\overline{d}} = &\frac{g^2 N_c}{32\pi m_W^2}|V_{ub}|^2 m_{H^{\pm}}\lambda^{1/2}(1, r_u, r_d)\\ &\times\left[(1-r_u-r_d)\left(m_u^2\cot^2\beta + m_d^2\tan^2\beta\right) - 4m_u m_d\right],\end{aligned} \tag{4.12}$$

where $r_i = m_i^2/m_{H^{\pm}}^2$ and N_c is the number of colours (3 for quarks, 1 for leptons). For a light $H^{\pm}$, one might naively expect the dominant decay at high $\tan\beta$ to be $H^+ \to c\overline{b}$, but due to the smallness of V_{cb}, this mode is suppressed with respect to leptonic decays. For a lepton pair, equation (4.12) can be further simplified into

$$\Gamma_{H^+\to\ell^+\nu_\ell} = \frac{g^2}{32\pi m_W^2} m_{H^{\pm}} m_\ell^2 \tan^2\beta. \tag{4.13}$$

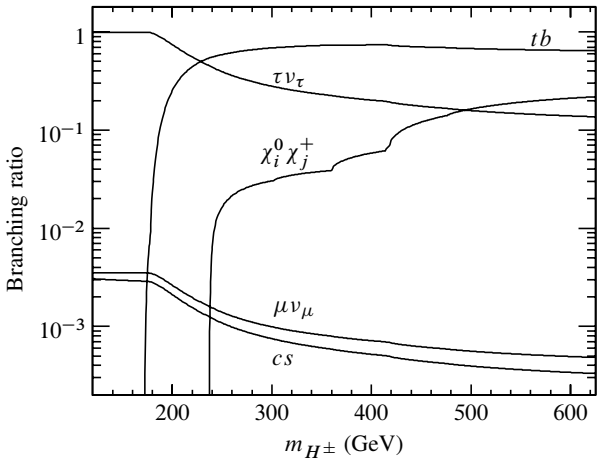

Figure 4.6: Decay branching ratios of $H^\pm$ in the $m_h^{\max}$ scenario for $\tan\beta = 50$. The numerical results were obtained using the code `FeynHiggs` [68].

The widths for the leptonic modes will thus have the hierarchy $m_\tau^2 : m_\mu^2 : m_e^2$, which evaluates numerically to $1 : 3\times10^{-3} : 8\times10^{-8}$. It is therefore unlikely that any leptonic decay mode besides $H^\pm \to \tau^\pm\nu_\tau$ will be important at the LHC. For this mode, techniques have been developed [67] for separation between the $H^\pm$ decay and background from ordinary $W^\pm$ decay by determining the τ lepton polarization from its hadronic decay products. In the rest frame of the decaying mother, the τ is produced with opposite helicity for a spin-0 versus a spin-1 resonance.

When the $H^\pm \to tb$ mode opens up it quickly becomes dominant. Similarly to the width $\Gamma_{t\to bH^+}$ presented in equation (4.6), the leading order expression can be improved [61]. The corrections have basically the same origin as above, and we only quote the final result

$$\begin{aligned}\Gamma^{\text{MSSM}}_{H^+\to t\bar b} = &\frac{g^2 N_c}{32\pi m_W^2}|V_{tb}|^2 m_{H^\pm}(1-r_t)^2 \frac{\overline{m}_b^2(m_{H^\pm}^2)}{(1+\epsilon_b\tan\beta)^2}\tan^2\beta \\ &\times\left\{1+\frac{\alpha_s(m_t^2)}{\pi}\left[\frac{17}{3}+6r_t+r_t^2-\frac{16}{27}r_t^3\right.\right. \\ &\left.\left.+\left(-4r_t-\frac{10}{3}r_t^2-\frac{40}{9}r_t^3\right)\log r_t\right]\right\},\end{aligned} \tag{4.14}$$

valid at high $\tan\beta$ for $r_b = 0$. In figure 4.6 we show the branching ratios of $H^\pm$ in the $m_h^{\max}$ scenario for $\tan\beta = 50$. The relative importance of different decays into SM particles does not change much with varying $\tan\beta$ in the high range. For really low $\tan\beta \lesssim 1$, the mode $H^\pm \to cs$ could in principle become interesting, although such low $\tan\beta$ values are excluded in the MSSM by the negative LEP searches for the neutral Higgs bosons [30]. As we see from

figure 4.6, sparticle decay modes may also become relevant as $m_{H^\pm}$ is further increased, primarily the decays $H^\pm \to \chi_i^0 \chi_j^\pm$ when kinematically allowed. The total branching ratio into SUSY decay modes has a maximum for $\tan\beta \simeq 7$, where $\Gamma_{H^+ \to t\overline{b}}$ is smallest. Beyond the MSSM, decays into gauge- and Higgs bosons, such as $H^\pm \to W^\pm A$ or $H^\pm \to W^\pm h$, may have a branching ratio close to unity when open.

A model-independent limit $m_{H^\pm} > 39.6$ GeV can be extracted from the contribution of $Z \to H^+H^-$ to the Z^0 width [56]. Beyond this result, the available decay modes of the charged Higgs determine the strategies for direct searches. At LEP, where charged Higgs pairs could have been produced through $e^+e^- \to \gamma/Z \to H^+H^-$, negative searches were performed in the channels $H^\pm \to \tau^\pm \nu_\tau$, $H^\pm \to cs$, and $H^\pm \to W^\pm A$. The resulting sensitivities vary somewhat between the channels, but a lower limit for type II models is $m_{H^\pm} > 76.6$ GeV at 95% confidence level [57]. At the Tevatron, both experiments have searched for a light $H^\pm$ in top quark decays. CDF obtained the limit $\mathrm{BR}(t \to bH^+) \lesssim 0.4$ for $\mathrm{BR}(H^+ \to \tau^+\nu_\tau) = 1$ [69]. Assuming instead that the charged Higgs decays only into $c\overline{s}$, they obtain the stronger limit $\mathrm{BR}(t \to bH^+) \lesssim 0.1$ for 60 GeV $< m_{H^\pm} <$ 150 GeV (excluding the region around $m_{H^\pm} = m_W$) [70]. DØ has performed a combined search [71], where both the $H^+ \to c\overline{s}$ and $H^+ \to \tau^+\nu_\tau$ modes were considered. The resulting limits are centered around $\mathrm{BR}(t \to bH^+) \lesssim 0.2$ for $m_{H^\pm} < 150$ GeV, with some dependence on the relative importance of the two channels. DØ has also published a search for heavy $H^+ \to t\overline{b}$ [72], but the resulting limits are not stringent enough to constrain the MSSM parameter space at this point. For the LHC era, the general-purpose experiments ATLAS [73] and CMS [74] are both ready to search for charged Higgs bosons in the main channels discussed here.[4]

[4]The recent theses [75] of my experimental colleagues provide good references for further reading on the preparations for charged Higgs boson searches with ATLAS.

5. Low-energy $H^{\pm}$ phenomenology

> "There's a bit of the charged Higgs boson in all of us."
>
> www.sloganizer.net

As discussed in the previous chapter, there are several processes through which a charged Higgs boson can be produced directly at a high-energy collider experiment. In this chapter we shall instead focus on *indirect* effects of $H^{\pm}$ in experiments at lower energies. The charged Higgs boson plays a special role as a scalar charged current, since it can contribute to observables at tree-level even in theories which violate flavour minimally, changing the predictions relative to the Standard Model. In the MSSM with R-parity conservation, this is a unique property. Following a concise theory introduction, we discuss in this chapter some of the most popular observables from B-physics in the framework of the MSSM (2HDM type II) at high $\tan\beta$.

5.1 Theory introduction

A charged Higgs boson enters weak processes at the same level as $W^{\pm}$, changing flavour quantum numbers either by one or two units; so-called $\Delta F = 1$ and $\Delta F = 2$ processes in flavour physics language. In new physics scenarios respecting *minimal flavour violation* (MFV) [76], no flavour structure beyond the CKM matrix is present at the weak scale. We restrict the discussion here to MFV scenarios.

A thorough introduction to flavour physics in the quark sector is given in the recent review [77]. We follow their discussion closely in this section. The appropriate language to describe low-energy weak transitions is that of effective field theories.[1] Using the operator product expansion (OPE) [78], a generic S-matrix element for the $\Delta F = 1$ transition $i \to f$ is expanded according to

$$\langle f | \mathrm{i}S | i \rangle = \frac{4G_F}{\sqrt{2}} \sum_k C_k(\mu) \langle f | \mathcal{O}_k(\mu) | i \rangle + \dots \tag{5.1}$$

[1] For the remainder of this chapter, we use the term *full* theory when referring to the complete SM (or MSSM), in contrast to the *effective* theory constructed below the weak scale. In the effective theory all heavy particles are removed as dynamical degrees of freedom.

Here G_F is the Fermi constant, and the terms represented by dots are suppressed by powers of Q^2/m_W^2, where for example $Q \simeq m_b$ for the decay of a B meson. Since the initial and final states have not been specified, the remaining parts of equation (5.1) are taken to define the effective Hamiltonian

$$\mathcal{H}_{\text{eff}}^{\Delta F=1} = \frac{4G_F}{\sqrt{2}} \sum_k C_k(\mu)\mathcal{O}_k(\mu). \tag{5.2}$$

The effective Hamiltonian describes interactions by a set $\{\mathcal{O}_k\}$ of local dimension-six operators forming a complete basis for the OPE. C_k are the *Wilson coefficients*, which act as effective couplings. All the dependence on short-distance physics (in the SM and beyond) is contained in these coefficients which, in principle, can be calculated once and for all for any specific theory.

The origin of the scale dependence in equation (5.2) is that QCD corrections to amplitudes calculated with the operators $\mathcal{O}_k$ generate UV divergences which are not present in the full theory. These are removed by renormalization, introducing a dependence on the renormalization scale μ. Since the complete effective Hamiltonian should not depend on the renormalization scale, the Wilson coefficients must have a dependence on μ cancelling that of the operators. Matching the effective theory to the full theory at the scale $\mu \simeq m_W$, large logarithms of the type $\alpha_s^n \log(m_W/\mu)^n$ appear in the Wilson coefficients. Similar to the use of a running coupling, these may be resummed through the renormalization group. Renormalization will also induce mixing among the Wilson coefficients through off-diagonal entries in the anomalous dimension matrix. To summarize, determining the effective Hamiltonian at the particular scale Q of the process at hand is a four-step process:

1. Decide on a basis for the operators $\mathcal{O}_k$, as given by the quantum numbers of the initial and final states under consideration.
2. Determine initial values for the Wilson coefficients at the matching scale $\mu \simeq m_W$, by matching matrix elements calculated in the effective theory to those in the full theory to leading order in Q^2/m_W^2.
3. Calculate the anomalous dimension matrix which governs the evolution of the Wilson coefficients from the matching scale to the scale μ.
4. Evolve $C_k(\mu)$ from the matching scale down to the desired scale $\mu = Q$.

In practice, steps 2–4 of this scheme can only be performed perturbatively, i.e. to a specific order in α_s.

As a final point on the theory introduction, we return to the dependence on long-distance physics. For initial and/or final states containing hadrons, non-perturbative QCD enters through the matrix elements $\langle f|\mathcal{O}_k|i\rangle$ of the local quark operators in equation (5.1). These matrix elements must either be evaluated with some appropriate non-perturbative method, or parameterized from data. Specific examples are given in the following sections.

5.2 Radiative B decays

Radiative B meson decays, in particular the inclusive mode $B \to X_s\gamma$, are sensitive low-energy probes for the charged Higgs. Since the decay $B \to X_s\gamma$ proceeds through a FCNC, it can only be generated at the loop level in the SM. The same is true in a new physics scenario with MFV. The effective Hamiltonian for $\Delta B = 1$, $\Delta S = -1$ transitions, assuming top quark dominance, is given by

$$\mathcal{H}_{\text{eff}} = -\frac{4G_F}{\sqrt{2}} V_{ts}^* V_{tb} \sum_k C_k(\mu)\mathcal{O}_k(\mu). \tag{5.3}$$

A complete on-shell basis of operators for the effective Hamiltonian (5.3) is given [79] by the eight elements

$$\begin{aligned}
\mathcal{O}_1 &= \big(\overline{s}_L\gamma_\mu T^a c_L\big)\big(\overline{c}_L\gamma^\mu T^a b_L\big)\\
\mathcal{O}_2 &= \big(\overline{s}_L\gamma_\mu c_L\big)\big(\overline{c}_L\gamma^\mu b_L\big)\\
\mathcal{O}_3 &= \big(\overline{s}_L\gamma_\mu b_L\big)\big(\overline{q}\gamma^\mu q\big)\\
\mathcal{O}_4 &= \big(\overline{s}_L\gamma_\mu T^a b_L\big)\big(\overline{q}\gamma^\mu T^a q\big)\\
\mathcal{O}_5 &= \big(\overline{s}_L\gamma_\mu\gamma_\nu\gamma_\rho b_L\big)\big(\overline{q}\gamma^\mu\gamma^\nu\gamma^\rho q\big)\\
\mathcal{O}_6 &= \big(\overline{s}_L\gamma_\mu\gamma_\nu\gamma_\rho T^a b_L\big)\big(\overline{q}\gamma^\mu\gamma^\nu\gamma^\rho T^a q\big)\\
\mathcal{O}_7 &= \frac{e}{16\pi^2} m_b\big(\overline{s}_L\sigma^{\mu\nu} b_R\big)F_{\mu\nu}\\
\mathcal{O}_8 &= \frac{g_s}{16\pi^2} m_b\big(\overline{s}_L\sigma^{\mu\nu} T^a b_R\big)G^a_{\mu\nu}.
\end{aligned}$$

The operators with $\overline{q}q$ involve a sum over the active quarks, and T^a are the generators of $\mathrm{SU}(3)_C$ in the fundamental representation. The strong and electromagnetic couplings are denoted by g_s and e, respectively. It turns out to be convenient to introduce effective Wilson coefficients $C_i^{\text{eff}}(\mu) = T_{ij}C_j(\mu)$. The coefficients T_{ij} can then be chosen so that the leading order contribution to $b \to s\gamma$ is given only by the linear combination C_7^{eff}. To leading logarithmic accuracy, the renormalization of this quantity can be expressed in closed form:

$$\begin{aligned}
C_7^{\text{eff}}(\mu) =& \eta^{16/23} C_7(m_W) + \frac{8}{3}\left(\eta^{14/23} - \eta^{16/23}\right) C_8(m_W)\\
&+ \sum_{i=1}^{6} h_i \eta^{a_i} C_2(m_W),
\end{aligned} \tag{5.4}$$

with $\eta = \alpha_s(m_W)/\alpha_s(\mu)$. Numerical values for h_i and a_i are given in [79]. Using heavy quark effective theory (HQET), corrections (of order 10%) to the approximation $\Gamma(B \to X_s\gamma) \simeq \Gamma(b \to s\gamma)$ can be computed. For the partonic

states, the inclusive decay rate at leading order can be expressed [80] as

$$\frac{\Gamma(b\to s\gamma)}{\Gamma(b\to ce\overline{\nu}_e)} = \frac{|V_{ts}^* V_{tb}|^2}{|V_{cb}|^2}\frac{6\alpha}{\pi g(z)}|C_7^{\text{eff}}(\mu)|^2, \tag{5.5}$$

where $g(z) = 1 - 8z^2 + 8z^6 - z^8 - 24z^4 \ln z$ is the phase-space factor for the semi-leptonic decay ($z = m_c/m_b$). The normalization to $\Gamma(b \to ce\overline{\nu}_e)$ is introduced to cancel uncertainties from m_b and CKM matrix elements. The lowest order contributions $C_7^{(0)}(\mu)$ at the matching scale $\mu = m_W$ are given by diagrams like those in figure 5.1. In the presence of new physics, the different contributions add

$$C_k^{(0)}(m_W) = C_k^{(0),\text{SM}}(m_W) + \delta C_k^{(0),H^\pm}(m_W) + \delta C_k^{(0),\text{MSSM}}(m_W). \tag{5.6}$$

Explicitly, the SM coefficients which are non-zero at leading order are given by

$$\begin{aligned}
C_2^{(0),\text{SM}}(m_W) &= 1,\\
C_{7,8}^{(0),\text{SM}}(m_W) &= F_{7,8}^{(1)}(x),\\
F_7^{(1)}(x) &= \frac{x(7-5x-8x^2)}{24(x-1)^3} + \frac{x^2(3x-2)}{4(x-1)^4}\log x,\\
F_8^{(1)}(x) &= \frac{x(2+5x-x^2)}{8(x-1)^3} - \frac{3x^2}{4(x-1)^4}\log x,
\end{aligned}$$

with $x = \overline{m}_t^2(m_W)/m_W^2$. To include the charged Higgs contribution, shown in figure 5.1, we only need to modify the Wilson coefficients by adding new terms. For the 2HDM type II (MSSM), we have

$$\begin{aligned}
\delta C_{7,8}^{(0),H^\pm}(m_W) &= \frac{\cot^2\beta}{3}F_{7,8}^{(1)}(y) + F_{7,8}^{(2)}(y),\\
F_7^{(2)}(y) &= \frac{y(3-5y)}{12(y-1)^2} + \frac{y(3y-2)}{6(y-1)^3}\log y,\\
F_8^{(2)}(y) &= \frac{y(3-y)}{4(y-1)^2} - \frac{y}{2(y-1)^3}\log y,
\end{aligned}$$

where now $y = \overline{m}_t^2(m_W)/m_{H^\pm}^2$. The contributions to $\delta C_{7,8}^{(0),\text{MSSM}}$ from exchange of charginos and squarks can be expressed in a similar fashion, but since the expressions become quite lengthy we omit them here. They can be found for example in [81]. An important result for $B \to X_s\gamma$ is that, while the $H^\pm$ contribution is always positive, the sparticle contributions may be of either sign. It is therefore quite possible to achieve a complete cancellation of the new physics contributions for certain parameter values in the MSSM.

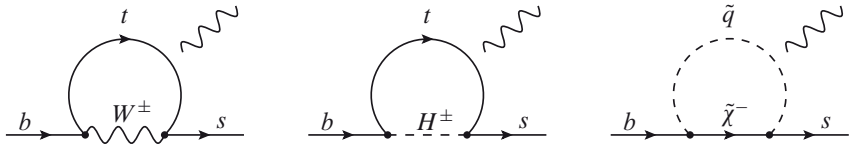

Figure 5.1: Contributions to $b \to s\gamma$ transitions in the SM (left), from a charged Higgs boson (centre), and from charginos and squarks (right). The loose photon is to be attached in all possible positions.

The precision calculation of $B \to X_s\gamma$ to higher orders in perturbation theory is a big industry. The expressions used in practical applications, e.g. for our own papers I and IV, go beyond the leading order description given here. In the Standard Model, the complete result is known at next-to-next-to-leading order (NNLO) [82]. Beyond the SM, the NLO contributions to the Wilson coefficients are known both for the charged Higgs contribution in the general 2HDM [83], and for the MSSM with minimal flavour violation [81].

5.3 Leptonic and semi-leptonic B decays

Leptonic and semi-leptonic decays of heavy quarks are processes where the charged Higgs can contribute significantly already at tree-level. In the MSSM with R-parity conservation, the charged Higgs provides the *only* new physics contribution of this type. The presence of a leptonic current makes the calculation of these observables much simpler than $b \to s\gamma$, and the QCD corrections are minor.

At large $\tan\beta$, the effective Hamiltonian mediating the transitions $bq \to \ell\nu_\ell$ and $b \to q\ell\nu_\ell$ ($q = u, c$) is given by [84]

$$\begin{aligned}\mathcal{H}_{\text{eff}} = \frac{G_F}{\sqrt{2}} V_{qb} \Big[&\Big(\overline{q}\gamma_\mu(1-\gamma_5)b\Big)\Big(\overline{\ell}\gamma^\mu(1-\gamma_5)\nu_\ell\Big) \\ &+ C_{H^\pm}(\mu)\Big(\overline{q}(1+\gamma_5)b\Big)\Big(\overline{\ell}(1-\gamma_5)\nu_\ell\Big)\Big] + \text{h.c.}\end{aligned} \tag{5.7}$$

The effective coupling of the scalar currents is expressed from the parameters entering the fundamental charged Higgs coupling as

$$C_{H^\pm}(\mu) = -\frac{\overline{m}_b(\mu) m_\ell}{m_{H^\pm}^2} \frac{\tan^2\beta}{1+\epsilon_b \tan\beta}. \tag{5.8}$$

Renormalization group evolution of $C_{H^\pm}(\mu)$ amounts to evaluating the $\overline{\text{MS}}$ quark mass at the scale μ where the corresponding quark current is defined. The non-holomorphic corrections ϵ_b appearing in equation (5.8) are the same as discussed previously in chapter 4.

Non-perturbative QCD effects arise also in leptonic and semi-leptonic hadron decays, from the coupling of the quark current to the hadronic state. In the case of a single hadron, the matrix elements can be parameterized in terms of a decay constant. For $B_u \to \ell\nu_\ell$, we are for example interested in

$$\begin{aligned}\langle 0|\overline{u}\gamma_5 b\,|B^-(p)\rangle &= -\mathrm{i}\,f_B\frac{m_B^2}{\overline{m}_b}\\ \langle 0|\overline{u}\gamma^\mu\gamma_5 b\,|B^-(p)\rangle &= \mathrm{i}\,f_B\,p^\mu.\end{aligned}$$

The B decay constant f_B must be extracted from data, or calculated using non-perturbative methods such as lattice QCD. For processes involving two hadrons, the single decay constant is replaced by form factors which depend on the kinematics. In the case of $\overline{B} \to D(\ell\nu_\ell)$, which we discuss below, we have the parameterization [85]

$$\begin{aligned}\langle D(p_D)|\overline{c}b\,|\overline{B}(p_B)\rangle &= \frac{m_B^2-m_D^2}{\overline{m}_b-\overline{m}_c}F_S(q^2)\\ \langle D(p_D)|\overline{c}\gamma^\mu b\,|\overline{B}(p_B)\rangle &= F_V(q^2)\left(p_B^\mu+p_D^\mu-\frac{m_B^2-m_D^2}{q^2}q^\mu\right)\\ &\quad + F_S(q^2)\frac{m_B^2-m_D^2}{q^2}q^\mu.\end{aligned}$$

The form factors $F_S(q^2)$ and $F_V(q^2)$ depend on the momentum transfer $q = p_B - p_D$. Like f_B, they must be determined from measurements or using non-perturbative methods.

From the effective Hamiltonian (5.7) and the hadronic matrix elements, one determines [86] the leptonic decay width

$$\Gamma_{B^\pm\to\ell^\pm\nu_\ell} = \frac{G_F^2|V_{ub}|^2 f_B^2 m_B}{8\pi}m_\ell^2\left(1-\frac{m_\ell^2}{m_B^2}\right)R_{\ell\nu}. \tag{5.11}$$

The charged Higgs contribution is contained in the factor

$$R_{\ell\nu} = \left(1-\frac{m_B^2}{m_{H^+}^2}\frac{\tan^2\beta}{1+\epsilon_b\tan\beta}\right)^2. \tag{5.12}$$

The $B^\pm \to \ell^\pm\nu_\ell$ decay width has several interesting properties. First of all, the contribution from $W^\pm$ exchange is proportional to m_ℓ^2, which signals helicity suppression. This makes the partial width small. The charged Higgs contribution suffers no helicity suppression, but the effective coupling – introduced in equation (5.8) – has an explicit dependence on m_ℓ. Hence the factor $R_{\ell\nu}$ is independent of the lepton mass, and the charged Higgs contributes an equal scaling factor for each lepton flavour. We also see from equation (5.12) that,

unless $\tan\beta$ is very large, the $R_{\ell\nu}$ factor will *reduce* the width in the presence of $H^\pm$ compared to the Standard Model expectation.

The second class of decays we are going to consider here are the semi-leptonic modes $B^\pm \to D\ell^\pm\nu_\ell$, which also derive from equation (5.7). In the notation of [87], the differential decay width is given by

$$\begin{aligned}\frac{\mathrm{d}\Gamma}{\mathrm{d}w} =& \frac{G_F^2|V_{cb}|^2 m_B^5}{192\pi^3}\rho_V(w) \\ &\times\left[1-\frac{m_\ell^2}{m_B^2}\left(1-\frac{t(w)}{m_{H^\pm}^2}\frac{\overline{m}_b}{\overline{m}_b-\overline{m}_c}\frac{\tan^2\beta}{1+\epsilon_b\tan\beta}\right)^2\rho_S(w)\right],\end{aligned} \tag{5.13}$$

where $t(w) = m_B^2 + m_D^2 - 2wm_Bm_D$, and the kinematic variable $w = v_B \cdot v_D = (m_B^2 + m_D^2 - q^2)/(2m_Bm_D)$ has been introduced. The partial width is obtained from equation (5.13) by integrating over the full kinematic range, including the dependence on the non-perturbative form factors $\rho_V(w)$ and $\rho_S(w)$ which have absorbed the functions called $F_S(q^2)$ and $F_V(q^2)$ above. Expressions for these form factors have been extracted previously both from lattice QCD [87], and from a combination of HQET and data [84]. Similarly to the purely leptonic decay, we observe that the widths for the semi-leptonic modes are reduced by the $H^\pm$ contribution for reasonable values of the effective coupling $C_{H^\pm}$. Since there is no helicity suppression of the SM contribution to this observable, a substantial charged Higgs influence is expected only for $B^\pm \to D\tau^\pm\nu_\tau$. The other modes can therefore be used for normalization, reducing the uncertainties. Beyond the branching ratio, the differential distribution of final state particles in the three-body decay contains information about the structure of the effective Hamiltonian. This is a promising channel to disentangle the contributions of $W^\pm$ and $H^\pm$ [84]. However, to do so will require more statistics than what is currently available.

The observables discussed in this chapter – together with several others – have been employed in papers I, II (for constrained versions of the MSSM) and IV, V (for the general 2HDM) to obtain constraints on the charged Higgs boson mass and couplings.

6. Cosmic neutrino detection

> "Fly me to the Moon, let me play among the stars."
>
> Bart Howard

This chapter provides introduction to the second topic of this thesis – cosmic neutrino detection. We begin with a short overview of cosmic neutrino sources, followed by some general aspects of high-energy neutrino detection, connecting to the primary detection method based on optical Cherenkov light. Finally, we introduce radio detection using the Askaryan effect, and discuss the current status of this method. This technique is considered in papers VIII and IX, where we determine the prospects for detection of radio signals from neutrinos interacting with the Moon.

6.1 Ultra-high-energy cosmic neutrinos

With cosmic neutrinos, we mean neutrinos which originate from outside the solar system. To date, the only cosmic neutrinos that have been detected are those which appeared in conjunction with the supernova SN1987A. Nevertheless, the measured spectrum of cosmic ray protons – with energy extending up to 10^{20} eV [18] – suggests an accompanying flux of neutrinos from the same sources. If detected, these neutrinos could aid in solving the puzzle associated with the sources of the highest energy cosmic rays. In the following, we shall refer generically to any neutrino with primary energy $E_\nu > 10^{17}$ eV as an *ultra-high-energy* (UHE) neutrino.[1]

With the new generation of experiments, neutrinos hold the promise of extending astronomy to an energy regime where photons can no longer reach the Earth due to absorption. Being electrically neutral, the neutrinos – like photons – make good astronomical messengers since they propagate undeflected through the cosmic magnetic fields. Astrophysical objects which can be primary sources for UHE particles are in principle anything with a strong enough magnetic field to accelerate charged particles effectively, see [88] for a review. The most prominent candidates, believed to produce particles with the highest

[1] Unless noted otherwise, energy quantities given in this chapter refer to the fixed-target ('lab') system with a nucleon target. Hence $E_\nu = 10^{17}$ eV corresponds to $E_{\mathrm{CM}} = \sqrt{2E_\nu m_p} \simeq 14$ TeV, i.e. the design energy of the LHC.

energy, are *Active Galactic Nuclei* (AGN), which are most likely galaxies with an accreting super-massive black hole in their centre.

Another source of UHE neutrinos deemed likely to exist is due to the Greisen-Zatsepin-Kuzmin (GZK) cutoff [89]. When the energy of a cosmic ray proton exceeds $E_{\mathrm{GZK}} \simeq 4 \times 10^{19}$ GeV, it can scatter resonantly on the cosmic microwave background photons (at $T = 2.7$ K) through

$$p + \gamma \to \Delta^{+}(1232) \to N\pi. \tag{6.1}$$

This interaction, which is well-studied from accelerator experiments, rapidly increases the attenuation of protons. It makes the universe opaque over length scales of tens of Mpc, thus setting the fundamental limit for cosmic ray astronomy. For many years, a controversy has existed related to the GZK cutoff, with several events reported to have a measured energy above the proposed limit [90]. However, this apparent paradox may now be resolved, as the recently measured deficit in the cosmic ray flux is compatible with the predicted cutoff [91]. An independent confirmation of these results would be the detection of the associated GZK neutrinos, which should be produced in the decay chain of charged pions

$$\pi^{+} \to \mu^{+}\nu_{\mu} \to e^{+}\nu_{e}\overline{\nu}_{\mu}\nu_{\mu}. \tag{6.2}$$

Assuming that the muon does not lose a large fraction of its energy before decaying, the average energy will be approximately equal among the leptons, and all three neutrinos in the final state contribute to the flux. This leads to a neutrino flux Φ_{ν} at the source with the flavour fractions $\Phi_{\nu_e} : \Phi_{\nu_\mu} : \Phi_{\nu_\tau} = 1 : 2 : 0$.[2] The initial flux composition will be modified by neutrino oscillations. By the time the neutrinos reach the Earth, the fractions are expected to be $\Phi_{\nu_e} : \Phi_{\nu_\mu} : \Phi_{\nu_\tau} = 1 : 1 \pm 0.15 : 1 \pm 0.15$ [92], where the uncertainties come from the neutrino mixing parameters. Since the pion decay chain, equation (6.2), is also the main source of neutrinos from cosmic rays accelerated in the magnetic field of an astrophysical object, the same flavour composition is expected for such neutrinos.

An alternative, more speculative, source of UHE neutrinos are *top-down* models. The common feature of these models is that they contain super-massive ($M_X \gtrsim 10^{22}$ eV) objects, which produce UHE particles through decay or annihilation [93]. These decays may allow the possibility for super-GZK energy cosmic rays and an accompanying neutrino flux, possibly with an energy spectrum extending up to the grand unification scale. Explicit examples of top-down models suggested in the literature involve various forms of topological defects, such as magnetic monopoles, cosmic string domain walls, or super-heavy forms of dark matter. It should however be mentioned that many of these top-down models are experimentally

[2]We have assumed that there is no experimental sensitivity to distinguish ν_ℓ from $\overline{\nu}_\ell$. This is indeed the case for the detection method we are going to discuss.

disfavoured by the recent Auger results [94] on the photon fraction in the UHE cosmic rays.

A phenomenological twist to explain the origin of the UHE cosmic rays is the proposal that they are produced locally, by UHE neutrinos annihilating with cosmological relic neutrinos at the Z pole, i.e. $\nu\overline{\nu} \to Z \to$ hadrons [95]. This process, called a Z-burst, requires a large abundance of neutrinos with $E_\nu \simeq 10^{21}$ eV, the origin of which is not explained. Even if this idea in itself does not suggest where the UHE neutrinos should come from in the first place, the necessary flux can be predicted and confronted with experiment.

6.2 Neutrino interactions and detection

Neutrinos interact with bulk matter only through the weak interaction. The feeble strength of this interaction makes them undetectable in collider experiments, where missing transverse momentum signatures are generated in the detectors. The interaction length for a neutrino passing through nuclear matter of density ρ can be expressed as

$$L_\nu = \frac{A}{N_A N \sigma_{\nu N} \rho}, \tag{6.3}$$

where A is the atomic mass number for the target nuclei which contain N nucleons, N_A is Avogadro's number, and $\sigma_{\nu N}$ the neutrino-nucleon cross section. In the SM, $\sigma_{\nu N}$ is a slowly increasing function of the primary energy, scaling roughly as $\sim E_\nu^{0.4}$ for $E_\nu > 10^{16}$ eV [96]. The ultra-high-energy cross section is dominated by contributions from partons at very small x, where the parton distributions are poorly constrained. The resulting uncertainty could reach a factor two or more for $E_\nu > 10^{20}$ eV. When $E_\nu > 10^{15}$ eV, the neutrino interaction length is shorter than the diameter of the Earth, which then starts to become opaque to neutrinos.

The deep inelastic scattering of a high-energy neutrino on a nucleon target proceeds either through a charged or a neutral current, as illustrated in figure 6.1. These interactions have distinct features which are employed for neutrino detection. In both cases, a hadronic shower is initiated by the energy transferred to the target. We shall return to the importance of this shower in the next section when we discuss radio methods. For the charged current, there is a charged lepton in the final state. The primary concept for cosmic neutrino detection relies on the final state muons produced in ν_μ events. The muons, being minimum ionizing particles, will travel a long distance in the detector medium while continuously emitting Cherenkov light. Instrumenting the detector volume with photo multiplier tubes the muons can be tracked, giving access to the original neutrino direction. The total light yield is used to measure the primary neutrino energy. Detection of ν_e and ν_τ is possible

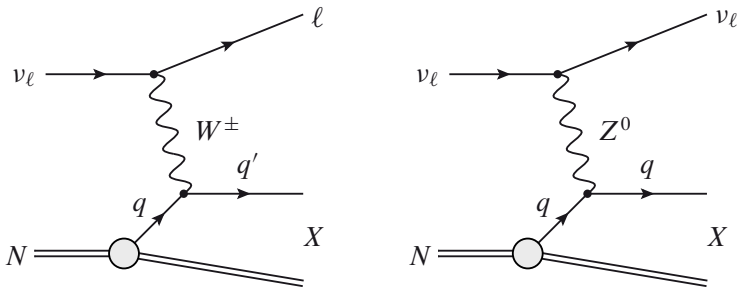

Figure 6.1: Deep inelastic neutrino scattering on a nucleon target N through charged current (left) and neutral current (right) weak interactions. X denotes a generic hadronic system which includes both the struck parton and the target remnant.

using essentially the same method, but the light deposition is more local and the direction sensitivity therefore somewhat worse.

Due to the low probability of a neutrino interaction taking place inside the detector material – and the expected very low flux of UHE neutrinos – a giant detector volume is necessary. The feasibility to use the Antarctic ice sheet as detection medium was first demonstrated by AMANDA [97], which has now been succeeded by IceCube [98]. The full IceCube detector will make use of 1 km^3 of the clear South Pole ice. This volume is instrumented with 80 strings, holding a total of 4800 digital optical modules with photo-multiplier tubes. In the northern hemisphere, the ANTARES experiment [99] complements IceCube by a similar (smaller) setup in the Mediterranean sea.

6.3 Radio detection

In the previous section, we sketched how neutrinos can be detected from the Cherenkov light emitted by the secondary lepton in a charged current interaction. At ultra-high energies, a viable alternative method is to detect the bulk of the shower. The hadronic shower, created both from the charged and neutral current interactions, contains a fraction $E = yE_\nu$ of the total energy, with $\langle y \rangle \simeq 0.2$ for the highest energy events [96]. The energy in the hadronic component will rapidly feed into electromagnetic sub-showers (mainly through $\pi^0 \to 2\gamma$ decay). The hadronic shower of an UHE event would appear in a neutrino telescope as an intense 'splash' of energy, allowing for a discovery and perhaps an energy measurement if the event is well-contained. Unfortunately, most models predict an UHE neutrino flux too low to be discovered even with a km^3 detector. This is where the radio methods enter.

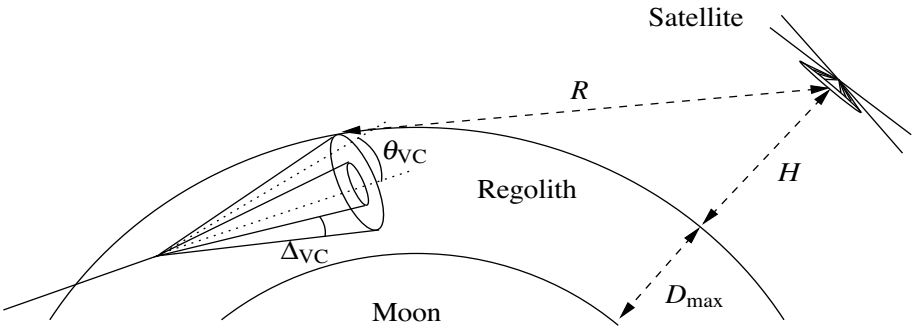

Figure 6.2: Sketch of the geometry (not to scale) for satellite detection of radio pulses from the Moon, induced by the interaction of an ultra-high-energy neutrino.

An initially neutral shower[3] evolving in a dielectric material develops a negative charge excess from secondary scattering processes with material electrons, known as the *Askaryan effect* [100]. Monte Carlo simulations have shown [101] that the total charge asymmetry reaches

$$\frac{N_{e^-} - N_{e^+}}{N_{e^-} + N_{e^+}} \simeq 20\% \tag{6.4}$$

for a fully developed shower. A macroscopic net charge distribution propagating through the material will generate Cherenkov radiation. For wavelengths longer than the transverse dimensions of the shower,[4] the classical emission will be *coherent*. The corresponding maximum frequency is called ω_0. For a dense material, such as rock or ice, ω_0 is typically in the few GHz range. The advantage with a coherent process is that the radiated power scales with the total charge, and thereby with the total energy as $P \sim E^2$, in contrast to the $P \sim E$ scaling for an incoherent process (such as optical Cherenkov emission). Since the shower is not of infinite extent, the angular distribution of the radiation is not limited to the precise Cherenkov angle, but has a spread which depends on material properties and the frequency under consideration. The coherence condition is maintained to larger angles for lower frequencies. The radiated electric field is linearly polarized in the plane spanned by the observation direction and the axis of shower propagation.

One step towards a proof-of-concept for using the Askaryan effect to search for UHE neutrinos was taken at SLAC, where the generation of coherent radio emission from an initially neutral (photon) beam was verified in a series of experiments [102]. The target materials were ice and silica sand.[5] Following

[3]The net charge is (close to) zero, but the shower can of course contain charged particles.

[4]The transverse size of the shower is taken as the Molière radius r_M. A cylinder with this radius contains on average 90% of the charged particles in the shower.

[5]Silica sand was chosen to resemble the lunar regolith, i.e. the uppermost dusty layer of the Moon. It consists of single mineral grains and small rock fragments, fused together by meteoritic impacts. Silicates make up the most abundant minerals in the regolith.

the successful demonstration at accelerators, several experiments searching for Askaryan signals from UHE interactions have been performed. The efforts have concentrated mainly around two sufficiently large bodies of target material: the Moon[6] and the Antarctic ice sheet. The surface of the Moon has been observed with large radio telescopes by the Parkes [103], GLUE [104], and Kalyazin [105] experiments. For Antarctica, both the embedded array RICE [106], and the balloon-borne experiment ANITA [107] circling the ice sheet were employed. Results from the satellite experiment FORTE [108] were analysed for pulses from the ice sheet covering Greenland. No events have been observed, but these radio experiments provide the most stringent limits on the neutrino flux above $E_\nu > 10^{18}$ eV [107].

We have developed ideas of using a radio instrument on-board a satellite in orbit around the Moon to detect Askaryan radio pulses. The geometry is sketched in figure 6.2. A satellite experiment would have several advantages over those performed with Earth-based radio telescopes: i) being closer to the source, a lower primary energy can yield a sufficiently strong radio signal for detection, ii) it would be designed for a longer exposure than the typical hours (or in the best cases, days) collected at the multi-purpose radio telescopes, iii) the lunar environment is radio quiet – in particular the far side of the Moon which is shielded from anthropogenic sources. Our calculations (paper VIII) show that the approach with a lunar satellite could be sensitive to neutrinos with $E_\nu \gtrsim 10^{20}$ eV. Needless to say, there are many technical and economical hurdles to overcome before this idea could be put to practice. Another, more down-to-Earth approach, is discussed in paper IX. This paper determines the prospects of Askaryan neutrino detection with the Giant Metrewave Radio Telescope (GMRT), consisting of 30 steerable dish antennas. For an observation time of one month, we find that the collected exposure would be competitive, but at the prize of a high threshold energy.

To conclude this chapter, we emphasize the importance of the intense activity now taking place in the field of UHE neutrino (and cosmic ray) searches. The smoke is clearing up around the GZK scale, and neutrino astronomy might be a reality within the next few years. New windows on the universe enable great discoveries. Beyond the search for astrophysical or GZK neutrinos, this is also a way of keeping the door open for something new and unexpected to be unveiled at the cosmic frontier of high-energy physics.

[6]The original suggestion to use the Moon for this type of experiment goes back to the 1962 paper of Askaryan [100].

Summary in Swedish

The purpose of this chapter is to give a brief summary of the thesis in Swedish.

Fysik vid högenergifronten

Fenomenologiska studier av laddade Higgsbosoner och detektion av kosmiska neutriner

Partikelfysik är den gren av fysiken som behandlar naturens minsta beståndsdelar och de krafter som verkar mellan dessa. Enligt Heisenbergs osäkerhetsrelation $\Delta x \Delta p \sim \hbar$ krävs höga energier för att observera fenomen vid korta längdskalor. I experimentell partikelfysik används därför stora *partikelacceleratorer* för att kollidera t.ex. protoner med hög energi och studera de reaktioner som äger rum. Den teoretiska partikelfysiken syftar till att tolka dessa reaktioner i termer av fysik. Genom matematiska modeller och realistiska datorsimuleringar kan förutsägelserna av olika teorier testas mot data. Gränssnittet mellan teori och experiment kallas ofta för *fenomenologi*.

Partikelfysikens *standardmodell* är en mycket framgångsrik teori för att beskriva experimentella observationer. Teorins kvantitativa förutsägelser har verifierats till bättre noggrannhet än en procent. Matematiskt sett är standardmodellen en gaugeteori baserad på symmetrigruppen $\mathrm{SU}(3) \times \mathrm{SU}(2) \times \mathrm{U}(1)$. Den beskriver de starka, svaga och elektromagnetiska krafterna. Den starka växelverkan – baserad på den icke-Abelska gruppen $\mathrm{SU}(3)_C$ – är en obruten gaugeteori med masslösa gaugebosoner (gluoner). Det samma gäller inte i den elektrosvaga sektorn $\mathrm{SU}(2)_L \times \mathrm{U}(1)_Y$, där symmetrin är spontant bruten till $\mathrm{U}(1)_{\mathrm{EM}}$ genom *Higgsmekanismen*. Som en konsekvens av symmetribrottet är tre ($Z^0, W^\pm$) av de elektrosvaga kraftbärarna massiva; endast fotonen förblir masslös. Av de fyra frihetsgrader som introduceras för att bryta den elektrosvaga symmetrin återstår efter symmetribrottet blott en. Denna tros utgöra *Higgsbosonen*, vilken dock ej observerats. Higgsbosonens massa m_h är heller inte bestämd av teorin, utan måste fastställas experimentellt. Detta är den enda parameter i standardmodellen vars värde ännu är okänt. Tidigare mätningar vid LEP[1] begränsar det möjliga intervallet till $114\ \mathrm{GeV} < m_h < 186\ \mathrm{GeV}$

[1]LEP: Large Electron-Positron collider; en tidigare stor partikelkolliderare vid det europeiska laboratoriet CERN i Genève. Fyra experiment var aktiva vid LEP under åren 1989–2000.

på 95% konfidensnivå. I standardmodellen är materian uppbyggd av fermioner med spinn $1/2$. Dessa delas in i sex *kvarkar* (d,u), (s,c), (b,t) och sex *leptoner* (e^-,ν_e), (μ^-,ν_μ), (τ^-,ν_τ). Likt gaugebosonernas massor kan även fermionmassor genereras genom Higgsmekanismen.

Trots framgångarna med att beskriva data har standardmodellen kända begränsningar. Den beskriver t.ex. varken gravitationskraften eller den mörka materia som utgör drygt 20% av den totala energitätheten i universum. Ett problem av mer teoretisk natur är att kvantkorrektioner till Higgsmassan uppvisar kvadratiska divergenser. Detta innebär att teorins förutsägelser i vissa fall inte är stabila under små variationer av parametrarna, en egenskap som anses icke önskvärd i en fundamental teori. Att introducera supersymmetri – en symmetri mellan fermioner och bosoner – är ett populärt sätt att komma till rätta med de två sistnämnda problemen. I den *minimala supersymmetriska standardmodellen* (MSSM) fördubblas antalet partiklar jämfört med standardmodellen. Dessutom krävs för teoretisk konsistens att ytterligare en komplex Higgsdublett införs. Det elektrosvaga symmetribrottet resulterar då i fem Higgsbosoner (istället för en), varav tre (h,H,A) är elektriskt neutrala och ett par $(H^\pm)$ är laddade. Den laddade Higgsbosonen är karaktäristisk för modeller av det här slaget och dess upptäckt vore ett otvetydigt bevis för fysik bortom standardmodellen. Artiklarna I och II som presenteras i denna avhandling diskuterar möjligheterna att detektera laddade Higgsbosoner i olika begränsade versioner av MSSM vid LHC.[2]

Higgssektorn i MSSM är ett specifikt exempel på en sk två-Higgsdublettmodell (2HDM). Supersymmetrin begränsar formen på denna så att den – i sin enklaste form – beskrivs av endast två parametrar. Man kan emellertid tänka sig andra, mer generella, teorier bortom standardmodellen som innehåller två Higgsdubletter och samtidigt medger ett större antal fria parametrar. För att studera massrelationer, partikelsönderfall och precisionstester av Higgsbosonernas egenskaper i dessa utökade modeller har vi utvecklat datorprogrammet `2HDMC`. Programmet beskrivs i artikel III och är fritt tillgängligt för nedladdning.

Som undertiteln antyder är ett speciellt fokus för den här avhandlingen den laddade Higgsbosonen $H^\pm$. Vid LHC skulle denna kunna skapas genom i huvudsak två processer. Om $H^\pm$ har högre massa än toppkvarken (t) är den dominerande produktionsmekanismen $pp \to \overline{t}bH^+$. Om $H^\pm$ istället har lägre massa än t kan man se det som en tvåstegsprocess, där $pp \to t\overline{t}$ följs av sönderfallet $t \to bH^+$ (se figur). Tvärsnittet för produktion av $t\overline{t}$ vid LHC är stort, $\sigma_{pp\to t\overline{t}} \simeq 900$ pb, vilket beräknas leda till produktion av 10^7 toppkvarkspar per år. Detta utgör ett tillräckligt statistikt underlag för mätningar av toppkvarkarnas egenskaper. Den starka växelverkan förutsäger bland annat att deras spinn skall vara korrelerade; en mätning av spinnet för t (från dess sönderfallsprodukter) ger viss kännedom om spinnet för $\overline{t}$ och vice versa. Man

[2]LHC: Large Hadron Collider; världens kraftfullaste partikelaccelerator, byggd för att åstadkomma protonkollisioner med en total tyngdpunktsenergi $E = 14$ TeV.

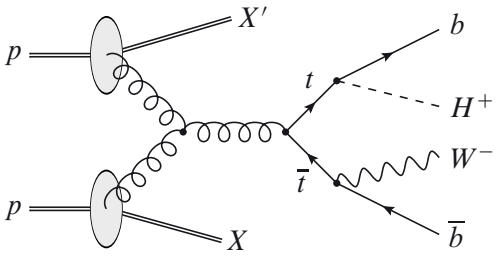

Figuren visar produktion av ett par toppkvarkar $t\bar{t}$ från två kolliderande protoner, följt av sönderfallen $t \to bH^+$ och $\bar{t} \to \bar{b}W^-$. Den laddade Higgsbosonen H^+ är en hypotetisk partikel som förutsägs av teorier bortom standardmodellen. Om den existerar är toppkvarksönderfall en möjlig process där den skulle kunna detekteras.

kan jämföra med situationen för den välkända EPR-paradoxen i kvantmekaniken. Vi har analyserat toppkvarkarnas spinnkorrelationer i kombination med sönderfallet $t \to bH^+$. Genom Monte Carlo-simuleringar har vi visat hur olika vinkelfördelningar i sluttillståndet kan användas för att bestämma strukturen på kopplingen tbH^+. Resultaten presenteras i artiklarna VI och VII.

Om en laddad Higgsboson existerar skulle den också kunna visa sig indirekt i processer vid lägre energi. Liksom $W^\pm$ utgör den en laddad ström som kan bidra till svaga sönderfall av exempelvis hadroner. Speciellt intressant är detta för sönderfall som beräknats vara sällsynta i standardmodellen, då man kan observera stora avvikelser från vad som förväntas. Eftersom styrkan på en partikels växelverkan med Higgsbosonerna är proportionell mot dess massa är det primärt för processer med tunga kvarkar, dvs B-mesoner, man kan förvänta sig de största effekterna. Exempel på en sådan process är det inklusiva sönderfallet $B \to X_s\gamma$ (X_s står för en godtycklig meson innehållande en s-kvark), som förutom ett bidrag från $H^\pm$ även är känsligt för utbyte av supersymmetriska partiklar. Andra intressanta sönderfall är $B^\pm \to \tau^\pm\nu_\tau$ och $B^\pm \to D\tau^\pm\nu_\tau$, där $H^\pm$ bidrar redan på trädnivå (lägsta ordningen i störningsteori). Vi har studerat dessa och andra liknande processer både för MSSM (i artikel I, II) och för mer generella 2HDM (artikel IV, V). Resultaten utgörs av gränser på den laddade Higgsbosonens massa och de värden som tillåts på kopplingarna för $H^\pm$ till kvarkar och leptoner i dessa modeller. Generellt finner vi att experiment vid låga energier utgör ett viktigt komplement till LHC och att dessa redan bidrar starkt till att begränsa parameterutrymmet för Higgsbosoner i teorier bortom standardmodellen.

Den andra delen av avhandlingen behandlar en speciell metod för detektion av ultrahögenergetiska kosmiska neutriner. Svårigheterna med att detektera dessa partiklar är dels att de är väldigt sällsynta, dels att de växelverkar mycket svagt med annan materia. Gigantiska detektorvolymer krävs därför. En metod för att åstadkomma detta bygger på den s.k. *Askaryaneffekten*. Denna föreslogs av Askaryan på 1960-talet, men har först under det senaste decenni-

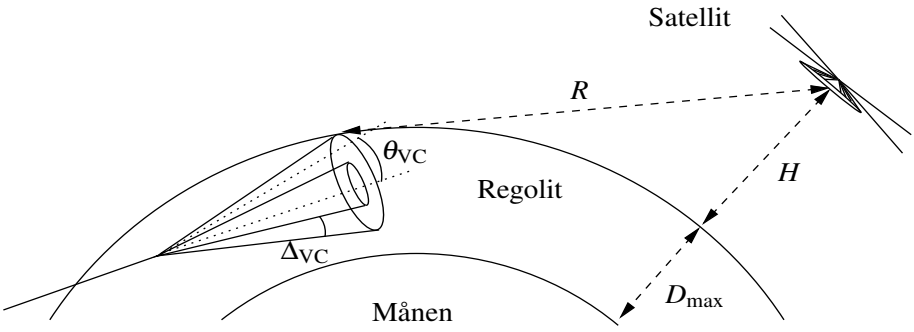

Bilden visar en (ej skalenlig) skiss över geometrin för neutrinodetektion från en månsatellit. En ultrahögenergetisk partikel kommer in från vänster och växelverkar med det övre lagret av månytan (regoliten). Den elektromagnetiska partikelskuren som uppkommer sänder ut radiostrålning. Signalen detekteras från en satellit som försetts med känslig radioutrustning.

et verifierats experimentellt. Askaryaneffekten kan kort beskrivas som att en partikelskur från en initial växelverkan (vid mycket hög energi) kommer att bygga upp ett överskott av negativ laddning då den propagerar genom ett tätt material. Detta sker genom successiva växelverkningar med materialet. Laddningsöverskottet kommer att avge Čerenkovstrålning. För våglängder längre än skurens transversella utsträckning (ca 10 cm i ett tätt material) kommer strålningen att vara *koherent*, dvs en primär energi E resulterar i en utstrålad effekt $P \sim E^2$ (till skillnad från en inkoherent process för vilken $P \sim E$).

Artikel VIII innehåller resultaten från en Monte Carlo-studie där vi undersökt möjligheterna att utnyttja Askaryanmetoden för att detektera kosmiska neutriner med radioutrustning på en satellit i omloppsbana kring månen. Månen utnyttjas då som måltavla för neutrinerna och en (eller företrädesvis flera) antenner söker efter signaler från månytan (se figur). Våra resultat visar att metoden framför allt är känslig för neutriner med energi $E_\nu > 10^{20}$ eV. Artikel IX presenterar en liknande studie vi gjort för det markbaserade radioteleskopet GMRT i Indien. Känsligheten hos teleskopet, som består av 30 antennelement, innebär en klar förbättring jämfört med tidigare experiment och står sig väl i konkurrensen även med framtida experiment vid de allra högsta energierna.

Flertalet av de projekt som redovisats här berör fysik vid de högsta energier som idag är tillgängliga. Frågeställningarna är ofta av karaktären: vad är möjligt med nästa generations experiment? Som avslutning vill jag därför framhålla att partikelfysiken nu står inför en mycket spännande tid. Vissa talar till och med om en gyllene tidsålder. Experimenten vid LHC kommer snart att börja leverera resultat om vad som döljer sig bortom standardmodellen. Parallellt går arbetet med detektion av kosmiska partiklar framåt i rasande fart. Avhandlingen är mitt eget blygsamma bidrag till denna fantastiska utveckling. Det är ett privilegium att få arbeta vid högenergifronten just idag.

Acknowledgements

Someone told me that the road to a PhD is long and perilous. Luckily, you meet a lot of helpful people along the way. I take this opportunity to express my gratitude towards those who have contributed indirectly to the publication of this thesis. I thank my earliest sources of inspiration first: my father – for sharing your passion for knowledge, and my mother – for teaching me how to get things done. Both qualities are equally important when writing a thesis.

It is a pleasure to thank a great high-school teacher, Sven-Erik Viberg, for encouraging my science interest. During my undergraduate studies, I benefited from 'Ångangänget' who took hard work and dedication to another level. Elias Coniavitis deserves my gratitude for promoting a science career – and for being such a good friend. I thank Bo Thidé for teaching, motivating me to enter science, and Jan Bergman for helping me develop further and supervising part of my work. My progress as a PhD student would not have been possible without the support and guidance from my excellent supervisors, Gunnar Ingelman and Johan Rathsman. Gunnar: you always believed in my potential and encouraged me to participate internationally. Johan: you provided ideas for new projects and answered my Higgs questions. I have enjoyed discussing different topics with both of you, and I really listen to your advice.

I thank my first office-mate David Eriksson for introducing me to many useful things – and for our good time working together. Next came Glenn Wouda, and we also created a nice atmosphere in a short time. I wish you good luck in the future. The THEP group has been a stimulating environment, owing much to the people coming in for longer or shorter periods of time: Emidio Gabrielli, Nazila Mahmoudi, Alexandre Arbey, Rikard Enberg, Roman Pasechnik, students and project workers. You have all been good colleagues. I am of course greatly indebted to my collaborators, not least our former postdoc Nazila. It was a pleasure working with you. The thesis itself has benefited from comments and discussions with the THEP group members plus Allan Hallgren, Olga Botner, Martin Flechl, Elias Coniavitis, and Nazila Mahmoudi.

My gratitude extends to all past and present colleagues and friends making my time at the department both productive and enjoyable. In addition to those already acknowledged, I thank Camille, Charlie, Enzo, Mathias, Bjarte, Claus, Richard, Tord Ekelöf, Karin, Patrik, Sophie, Pär-Anders, Erik, Agnes, Peder, Magnus, Henrik J, Henrik P, Anna, Johan L, Olle, Tord J, Inger, and Annica. The anonymous technician responsible for the coffee machine is recognized for countless moments of happiness.

Last – but not least – my most sincere thanks to my friends, to my wonderful family, and to my supportive wife Maria for your patience. I love you.

Bibliography

[1] C.-N. Yang and R. L. Mills *Phys. Rev.* **96** (1954) 191–195.

[2] R. P. Feynman *Rev. Mod. Phys.* **20** (1948) 367–387.

[3] L. D. Faddeev and V. N. Popov *Phys. Lett.* **B25** (1967) 29–30.

[4] T. van Ritbergen, J. A. M. Vermaseren, and S. A. Larin *Phys. Lett.* **B400** (1997) 379–384, [hep-ph/9701390].

[5] D. J. Gross and F. Wilczek *Phys. Rev. Lett.* **30** (1973) 1343–1346; H. D. Politzer *Phys. Rev. Lett.* **30** (1973) 1346–1349.

[6] V. N. Gribov and L. N. Lipatov *Sov. J. Nucl. Phys.* **15** (1972) 438–450; G. Altarelli and G. Parisi *Nucl. Phys.* **B126** (1977) 298; Y. L. Dokshitzer *Sov. Phys. JETP* **46** (1977) 641–653.

[7] S. L. Glashow *Nucl. Phys.* **22** (1961) 579–588; S. Weinberg *Phys. Rev. Lett.* **19** (1967) 1264–1266; A. Salam in *Elementary particle theory, proceedings of the Nobel Symposium held 1968 at Lerum, Sweden* (N. Svartholm, ed.), pp. 367–377, 1968.

[8] G. 't Hooft *Nucl. Phys.* **B35** (1971) 167–188; G. 't Hooft and M. J. G. Veltman *Nucl. Phys.* **B44** (1972) 189–213.

[9] P. W. Higgs *Phys. Lett.* **12** (1964) 132–133; F. Englert and R. Brout *Phys. Rev. Lett.* **13** (1964) 321–322; P. W. Higgs *Phys. Rev. Lett.* **13** (1964) 508–509.

[10] LEP Electroweak working group. Results published online, summer 2009 update: http://lepewwg.web.cern.ch/LEPEWWG/.

[11] LEP Working Group for Higgs boson searches, R. Barate *et. al. Phys. Lett.* **B565** (2003) 61–75, [hep-ex/0306033].

[12] The TEVNPH Working Group arXiv:0911.3930.

[13] N. Cabibbo *Phys. Rev. Lett.* **10** (1963) 531–533.

[14] M. Kobayashi and T. Maskawa *Prog. Theor. Phys.* **49** (1973) 652–657.

[15] C. Jarlskog *Phys. Rev. Lett.* **55** (1985) 1039.

[16] Super-Kamiokande collaboration, Y. Fukuda *et. al. Phys. Rev. Lett.* **81** (1998) 1562–1567, [hep-ex/9807003]; SNO collaboration, Q. R. Ahmad *et. al. Phys. Rev. Lett.* **89** (2002) 011301, [nucl-ex/0204008].

[17] T. Yanagida. In *Proceedings of the Workshop on Unified Theory and Baryon Number of the Universe*, eds. O. Sawada and A. Sugamoto (KEK, 1979) p.95.

[18] Particle Data Group collaboration, C. Amsler *et. al. Phys. Lett.* **B667** (2008) 1.

[19] M. J. G. Veltman *Acta Phys. Polon.* **B12** (1981) 437.

[20] S. Dimopoulos and G. L. Landsberg *Phys. Rev. Lett.* **87** (2001) 161602, [hep-ph/0106295].

[21] WMAP collaboration, D. N. Spergel *et. al. Astrophys. J. Suppl.* **148** (2003) 175–194, [astro-ph/0302209]; WMAP collaboration, E. Komatsu *et. al. Astrophys. J. Suppl.* **180** (2009) 330–376, [arXiv:0803.0547]; SDSS collaboration, M. Tegmark *et. al. Phys. Rev.* **D74** (2006) 123507, [astro-ph/0608632].

[22] J. Wess and B. Zumino *Phys. Lett.* **B49** (1974) 52; J. Wess and B. Zumino *Nucl. Phys.* **B70** (1974) 39–50; J. Wess and B. Zumino *Nucl. Phys.* **B78** (1974) 1.

[23] R. Haag, J. T. Lopuszanski, and M. Sohnius *Nucl. Phys.* **B88** (1975) 257.

[24] P. Fayet *Phys. Lett.* **B69** (1977) 489.

[25] L. Girardello and M. T. Grisaru *Nucl. Phys.* **B194** (1982) 65.

[26] J. R. Ellis, J. S. Hagelin, D. V. Nanopoulos, K. A. Olive, and M. Srednicki *Nucl. Phys.* **B238** (1984) 453–476.

[27] M. E. Peskin and D. V. Schroeder, *An Introduction to quantum field theory*. Westview Press, USA, 1995.

[28] J. F. Gunion, H. E. Haber, G. L. Kane, and S. Dawson, *The Higgs Hunter's Guide*. Perseus Publishing, Cambridge, MA, 2 ed., 1990.

[29] P. Skands *et. al. JHEP* **07** (2004) 036, [hep-ph/0311123].

[30] The LEP working group for Higgs boson searches *Eur. Phys. J.* **C47** (2006) 547–587, [hep-ex/0602042].

[31] Y. Okada, M. Yamaguchi, and T. Yanagida *Prog. Theor. Phys.* **85** (1991) 1–6; J. R. Ellis, G. Ridolfi, and F. Zwirner *Phys. Lett.* **B262** (1991) 477–484; H. E. Haber and R. Hempfling *Phys. Rev. Lett.* **66** (1991) 1815–1818.

[32] M. S. Carena *et. al. Nucl. Phys.* **B580** (2000) 29–57, [hep-ph/0001002].

[33] M. S. Carena and H. E. Haber *Prog. Part. Nucl. Phys.* **50** (2003) 63–152, [hep-ph/0208209].

[34] M. S. Carena, S. Heinemeyer, C. E. M. Wagner, and G. Weiglein hep-ph/9912223; M. S. Carena, S. Heinemeyer, C. E. M. Wagner, and G. Weiglein *Eur. Phys. J.* **C26** (2003) 601–607, [hep-ph/0202167].

[35] U. Amaldi, W. de Boer, and H. Furstenau *Phys. Lett.* **B260** (1991) 447–455.

[36] H. P. Nilles *Phys. Rept.* **110** (1984) 1–162.

[37] J. R. Ellis, K. A. Olive, Y. Santoso, and V. C. Spanos *Phys. Lett.* **B573** (2003) 162–172, [hep-ph/0305212].

[38] D. Matalliotakis and H. P. Nilles *Nucl. Phys.* **B435** (1995) 115–128, [hep-ph/9407251]; M. Olechowski and S. Pokorski *Phys. Lett.* **B344** (1995) 201–210, [hep-ph/9407404].

[39] S. Weinberg *Phys. Rev. Lett.* **37** (1976) 657.

[40] J. F. Gunion and H. E. Haber *Phys. Rev.* **D67** (2003) 075019, [hep-ph/0207010].

[41] H. E. Haber and R. Hempfling *Phys. Rev.* **D48** (1993) 4280–4309, [hep-ph/9307201].

[42] M. Dine, N. Seiberg, and S. Thomas *Phys. Rev.* **D76** (2007) 095004, [arXiv:0707.0005]; I. Antoniadis, E. Dudas, and D. M. Ghilencea *JHEP* **03** (2008) 045, [arXiv:0708.0383]; M. Carena, K. Kong, E. Ponton, and J. Zurita arXiv:0909.5434.

[43] I. F. Ginzburg and M. Krawczyk *Phys. Rev.* **D72** (2005) 115013, [hep-ph/0408011].

[44] S. Davidson and H. E. Haber *Phys. Rev.* **D72** (2005) 035004, [hep-ph/0504050].

[45] H. E. Haber and D. O'Neil *Phys. Rev.* **D74** (2006) 015018, [hep-ph/0602242].

[46] S. L. Glashow and S. Weinberg *Phys. Rev.* **D15** (1977) 1958.

[47] S. Frixione and B. R. Webber *JHEP* **06** (2002) 029, [hep-ph/0204244]; S. Frixione, P. Nason, and C. Oleari *JHEP* **11** (2007) 070, [arXiv:0709.2092].

[48] T. Sjöstrand *Phys. Lett.* **B157** (1985) 321.

[49] S. Catani, F. Krauss, R. Kuhn, and B. R. Webber *JHEP* **11** (2001) 063, [hep-ph/0109231].

[50] B. Andersson, G. Gustafson, G. Ingelman, and T. Sjöstrand *Phys. Rept.* **97** (1983) 31–145.

[51] T. Sjöstrand, S. Mrenna, and P. Skands *JHEP* **05** (2006) 026, [hep-ph/0603175]; T. Sjöstrand, S. Mrenna, and P. Skands *Comput. Phys. Commun.* **178** (2008) 852–867, [arXiv:0710.3820].

[52] G. Corcella *et. al. JHEP* **01** (2001) 010, [hep-ph/0011363]; G. Corcella *et. al.* hep-ph/0210213; M. Bahr *et. al. Eur. Phys. J.* **C58** (2008) 639–707, [arXiv:0803.0883].

[53] W. Bernreuther *J. Phys.* **G35** (2008) 083001, [arXiv:0805.1333].

[54] M. Cacciari, S. Frixione, M. L. Mangano, P. Nason, and G. Ridolfi *JHEP* **09** (2008) 127, [arXiv:0804.2800].

[55] G. Mahlon and S. J. Parke *Phys. Rev.* **D53** (1996) 4886–4896, [hep-ph/9512264]; T. Stelzer and S. Willenbrock *Phys. Lett.* **B374** (1996) 169–172, [hep-ph/9512292].

[56] DELPHI collaboration, J. Abdallah *et. al. Eur. Phys. J.* **C34** (2004) 399–418, [hep-ex/0404012].

[57] OPAL collaboration, G. Abbiendi *et. al.* arXiv:0812.0267.

[58] C. S. Li and T. C. Yuan *Phys. Rev.* **D42** (1990) 3088–3092; M. Drees and D. P. Roy *Phys. Lett.* **B269** (1991) 155–160; C.-S. Li, Y.-S. Wei, and J.-M. Yang *Phys. Lett.* **B285** (1992) 137–140; A. Czarnecki and S. Davidson *Phys. Rev.* **D48** (1993) 4183–4187, [hep-ph/9301237].

[59] E. Braaten and J. P. Leveille *Phys. Rev.* **D22** (1980) 715; M. Drees and K.-I. Hikasa *Phys. Lett.* **B240** (1990) 455.

[60] L. J. Hall, R. Rattazzi, and U. Sarid *Phys. Rev.* **D50** (1994) 7048–7065, [hep-ph/9306309].

[61] M. S. Carena, D. Garcia, U. Nierste, and C. E. M. Wagner *Nucl. Phys.* **B577** (2000) 88–120, [hep-ph/9912516].

[62] F. Borzumati, J.-L. Kneur, and N. Polonsky *Phys. Rev.* **D60** (1999) 115011, [hep-ph/9905443]; S. Moretti and D. P. Roy *Phys. Lett.* **B470** (1999) 209–214, [hep-ph/9909435].

[63] J. Alwall and J. Rathsman *JHEP* **12** (2004) 050, [hep-ph/0409094].

[64] S.-h. Zhu *Phys. Rev.* **D67** (2003) 075006, [hep-ph/0112109].

[65] T. Plehn *Phys. Rev.* **D67** (2003) 014018, [hep-ph/0206121]; E. L. Berger, T. Han, J. Jiang, and T. Plehn *Phys. Rev.* **D71** (2005) 115012, [hep-ph/0312286].

[66] S. Dittmaier, M. Kramer, M. Spira, and M. Walser arXiv:0906.2648.

[67] S. Raychaudhuri and D. P. Roy *Phys. Rev.* **D53** (1996) 4902–4908, [hep-ph/9507388].

[68] S. Heinemeyer, W. Hollik, and G. Weiglein *Comput. Phys. Commun.* **124** (2000) 76–89, [hep-ph/9812320]; S. Heinemeyer, W. Hollik, and G. Weiglein *Eur. Phys. J.* **C9** (1999) 343–366, [hep-ph/9812472]; G. Degrassi, S. Heinemeyer, W. Hollik, P. Slavich, and G. Weiglein *Eur. Phys. J.* **C28** (2003) 133–143, [hep-ph/0212020]; M. Frank *et. al. JHEP* **02** (2007) 047, [hep-ph/0611326].

[69] CDF collaboration, A. Abulencia *et. al. Phys. Rev. Lett.* **96** (2006) 042003, [hep-ex/0510065].

[70] CDF collaboration, T. Aaltonen *et. al. Phys. Rev. Lett.* **103** (2009) 101803, [arXiv:0907.1269].

[71] DØ collaboration, V. M. Abazov *et. al.* arXiv:0908.1811; DØ collaboration, V. M. Abazov *et. al. Phys. Rev.* **D80** (2009) 051107, [arXiv:0906.5326].

[72] DØ collaboration, V. M. Abazov *et. al. Phys. Rev. Lett.* **102** (2009) 191802, [arXiv:0807.0859].

[73] The ATLAS collaboration, G. Aad *et. al.* arXiv:0901.0512. Charged Higgs boson searches are described on p. 1451-1480 of this massive report.

[74] CMS collaboration, A. De Roeck *et. al. J. Phys.* **G34** (2006) 995–1579.

[75] M. Flechl, *Looking for the Charged Higgs Boson. Simulation Studies for the ATLAS Experiment*. PhD thesis, Uppsala University, 2010; E. Coniavitis, *Charged Higgs Bosons at the ATLAS Experiment and Beyond*. PhD thesis, Uppsala University, 2010. Electronic versions accessible from http://uu.diva-portal.org.

[76] A. J. Buras, P. Gambino, M. Gorbahn, S. Jager, and L. Silvestrini *Phys. Lett.* **B500** (2001) 161–167, [hep-ph/0007085]; G. D'Ambrosio, G. F. Giudice, G. Isidori, and A. Strumia *Nucl. Phys.* **B645** (2002) 155–187, [hep-ph/0207036].

[77] M. Antonelli *et. al.* arXiv:0907.5386.

[78] K. G. Wilson *Phys. Rev.* **179** (1969) 1499–1512.

[79] K. G. Chetyrkin, M. Misiak, and M. Munz *Phys. Lett.* **B400** (1997) 206–219, [hep-ph/9612313]. Erratum: *ibid.* **B425**, 414 (1998).

[80] A. J. Buras, M. Misiak, M. Münz, and S. Pokorski *Nucl. Phys.* **B424** (1994) 374–398, [hep-ph/9311345].

[81] M. Ciuchini, G. Degrassi, P. Gambino, and G. F. Giudice *Nucl. Phys.* **B534** (1998) 3–20, [hep-ph/9806308].

[82] M. Misiak *et. al. Phys. Rev. Lett.* **98** (2007) 022002, [hep-ph/0609232]; T. Becher and M. Neubert *Phys. Rev. Lett.* **98** (2007) 022003, [hep-ph/0610067].

[83] M. Ciuchini, G. Degrassi, P. Gambino, and G. F. Giudice *Nucl. Phys.* **B527** (1998) 21–43, [hep-ph/9710335].

[84] U. Nierste, S. Trine, and S. Westhoff *Phys. Rev.* **D78** (2008) 015006, [arXiv:0801.4938].

[85] U. Nierste *Nucl. Phys. Proc. Suppl.* **185** (2008) 195–200, [arXiv:0807.3733].

[86] W.-S. Hou *Phys. Rev.* **D48** (1993) 2342–2344.

[87] J. F. Kamenik and F. Mescia *Phys. Rev.* **D78** (2008) 014003, [arXiv:0802.3790].

[88] J. G. Learned and K. Mannheim *Ann. Rev. Nucl. Part. Sci.* **50** (2000) 679–749.

[89] K. Greisen *Phys. Rev. Lett.* **16** (1966) 748–750; G. Zatsepin and V. Kuzmin *JETP Lett.* **4** (1966) 78.

[90] N. Hayashida *et. al. Phys. Rev. Lett.* **73** (1994) 3491–3494.

[91] HiRes collaboration, R. Abbasi *et. al. Phys. Rev. Lett.* **100** (2008) 101101, [astro-ph/0703099]; Pierre Auger collaboration, J. Abraham *et. al. Phys. Rev. Lett.* **101** (2008) 061101, [arXiv:0806.4302].

[92] T. Kashti and E. Waxman *Phys. Rev. Lett.* **95** (2005) 181101, [astro-ph/0507599].

[93] P. Bhattacharjee, C. T. Hill, and D. N. Schramm *Phys. Rev. Lett.* **69** (1992) 567–570.

[94] Pierre Auger collaboration, J. Abraham *et. al. Astropart. Phys.* **31** (2009) 399–406, [arXiv:0903.1127].

[95] D. Fargion, B. Mele, and A. Salis *Astrophys. J.* **517** (1999) 725–733, [astro-ph/9710029]; T. J. Weiler *Astropart. Phys.* **11** (1999) 303–316, [hep-ph/9710431].

[96] R. Gandhi, C. Quigg, M. H. Reno, and I. Sarcevic *Astropart. Phys.* **5** (1996) 81–110, [hep-ph/9512364]; R. Gandhi, C. Quigg, M. H. Reno, and I. Sarcevic *Phys. Rev.* **D58** (1998) 093009, [hep-ph/9807264].

[97] AMANDA collaboration, E. Andres *et. al. Nature* **410** (2001) 441–443.

[98] IceCube collaboration, S. R. Klein *IEEE Trans. Nucl. Sci.* **56** (2009) 1141–1147, [arXiv:0807.0034].

[99] ANTARES collaboration, A. Margiotta *Nucl. Phys. Proc. Suppl.* **190** (2009) 121–126.

[100] G. A. Askaryan *Sov. Phys. JETP* **14** (1962) 441–443; G. A. Askaryan *Sov. Phys. JETP* **21** (1965) 658–659; G. A. Askaryan *JETP Lett.* **39** (1984) 402–405.

[101] E. Zas, F. Halzen, and T. Stanev *Phys. Rev.* **D45** (1992) 362–376.

[102] D. Saltzberg *et. al. Phys. Rev. Lett.* **86** (2001) 2802–2805, [hep-ex/0011001]; P. W. Gorham *et. al. Phys. Rev.* **D72** (2005) 023002, [astro-ph/0412128]; ANITA collaboration, P. W. Gorham *et. al. Phys. Rev. Lett.* **99** (2007) 171101, [hep-ex/0611008].

[103] C. W. James *et. al. Mon. Not. Roy. Astron. Soc.* **379** (2007) 1037–1041, [astro-ph/0702619].

[104] P. W. Gorham *et. al. Phys. Rev. Lett.* **93** (2004) 041101, [astro-ph/0310232].

[105] A. R. Beresnyak, R. D. Dagkesamansky, A. V. Kovalenko, V. V. Oreshko, and I. M. Zheleznykh *Astron. Rep.* **49** (2005) 127–133.

[106] I. Kravchenko *et. al. Phys. Rev.* **D73** (2006) 082002, [astro-ph/0601148].

[107] ANITA collaboration, P. W. Gorham *et. al. Phys. Rev. Lett.* **103** (2009) 051103, [arXiv:0812.2715]; ANITA collaboration, S. W. Barwick *et. al. Phys. Rev. Lett.* **96** (2006) 171101, [astro-ph/0512265].

[108] N. G. Lehtinen, P. W. Gorham, A. R. Jacobson, and R. A. Roussel-Dupre *Phys. Rev.* **D69** (2004) 013008, [astro-ph/0309656].

Acta Universitatis Upsaliensis

Digital Comprehensive Summaries of Uppsala Dissertations from the Faculty of Science and Technology 699

Editor: The Dean of the Faculty of Science and Technology

A doctoral dissertation from the Faculty of Science and Technology, Uppsala University, is usually a summary of a number of papers. A few copies of the complete dissertation are kept at major Swedish research libraries, while the summary alone is distributed internationally through the series Digital Comprehensive Summaries of Uppsala Dissertations from the Faculty of Science and Technology. (Prior to January, 2005, the series was published under the title "Comprehensive Summaries of Uppsala Dissertations from the Faculty of Science and Technology".)

Distribution: publications.uu.se
urn:nbn:se:uu:diva-111162

ACTA
UNIVERSITATIS
UPSALIENSIS
UPPSALA
2009